Review Article | Open Access

Soft Science

Wang *et al. Soft Sci.* **2026**, *6*, 8 **DOI:**10.20517/ss.2025.98

Recent advances in carbon-based microwave-absorbing aerogel

Kaifeng Wang[1,*], Wenshuang Chu[2], Xinke Liu[1], Xiaohua Li[1], Hezhou Liu[1]

Keywords:
Microwave absorption, carbon-based aerogel, porous structure, construction methods

Citation: Wang, K.; Chu, W.; Liu, X.; Li, X.; Liu, H. Recent advances in carbon-based microwave-absorbing aerogel. *Soft Sci.* **2026**, *6*, 8. https://dx.doi.org/10.20517/ss.2025.98

Received: 30 Sep 2025 **First Decision:** 11 Nov 2025 **Revised:** 8 Dec 2025 **Accepted:** 19 Dec 2025 **Published:** 21 Jan 2026

Academic Editor: YongAn Huang **Copy Editor:** Pei-Yun Wang **Production Editor:** Pei-Yun Wang

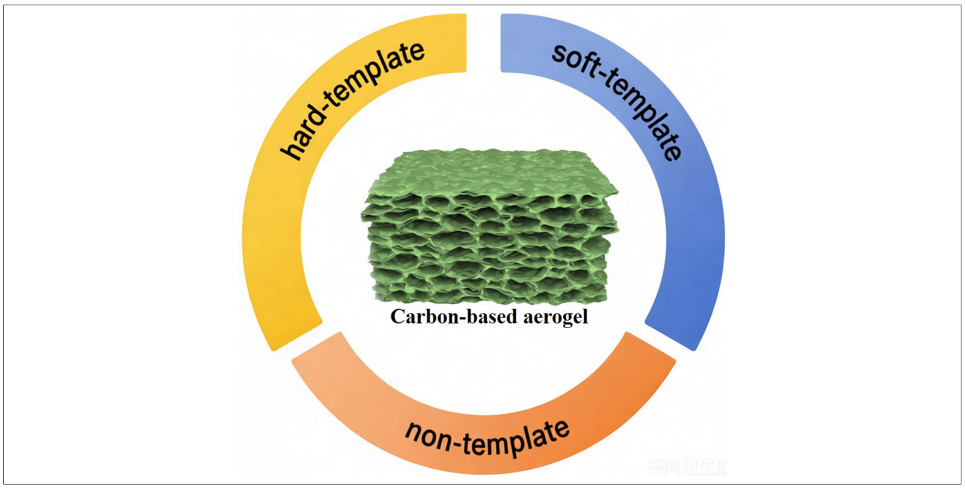

Abstract

Carbon-based microwave-absorbing (MA) aerogel materials have emerged as a prominent research focus in recent years due to their three-dimensional (3D) interconnected conductive networks and diverse porous microstructures, which optimize impedance matching and dissipate microwaves through multiple loss effects. Guided by the research rationale of constructing carbon-based aerogels with diverse microstructures and corresponding unique electromagnetic response behaviors, this review systematically summarizes recent advances in carbon-based microwave-absorbing aerogels over the past five years, with particular emphasis on the rational design of carbon-based aerogels using different templating strategies. These include hard-template methods based on natural biomass and polymer foams, soft-template approaches such as isotropic and directional freeze-drying, and non-template techniques such as electrospinning and 3D printing. By discussing the mechanisms and advantages of these synthesis strategies in depth, the relationship between porous architecture and microwave response properties is elucidated, while also providing insights and perspectives on future carbon-based microwave-absorbing aerogels with synergistic performance and potential for large-scale production.

[1]College of Materials Science and Engineering, Shenzhen University, Shenzhen 518060, Guangdong, China.
[2]Department of Chemistry, Tonghua Normal University, Tonghua 134002, Jilin, China.

Correspondence to: Dr. Kaifeng Wang, College of Materials Science and Engineering, Shenzhen University, Shenzhen 518060, Guangdong, China. E-mail: kfwang@szu.edu.cn

INTRODUCTION

The rapid advancement of fifth-generation (5G) communication technology has remarkably accelerated the proliferation and adoption of advanced electronic devices, bringing unprecedented convenience to modern society, while raising serious concerns over electromagnetic (EM) radiation[1-5]. EM pollution not only interferes with the precise operation of electronic equipment and signal transmission but also poses potential risks to human health, including chronic diseases and long-term physiological damage. Furthermore, in the military domain, radar stealth technology plays a critical role in defending against enemy detection systems and ensuring reliable satellite communication, which enhances the survivability on the battlefield. In this context, microwave-absorbing materials (MAMs) have emerged as a feasible solution to mitigate external EM radiation, demonstrating significant research value and broad application potential in both military defense and civilian fields.

Ideal MAMs should exhibit strong reflection loss (RL) intensity and a wide effective absorption bandwidth (EAB), which requires a combination of excellent impedance matching and sufficient EM attenuation capability. This combination allows microwaves to effectively penetrate the MAMs and be efficiently attenuated through energy conversion and dissipation mechanisms[6-10]. Conventional MAMs, such as ferrites, metal powders, and conductive polymers, often suffer from high density, limited RL intensity, narrow EAB, and unstable performance under complex conditions. Carbon-based materials, recognized as promising dielectric loss absorbers, provide advantages including high and tunable electrical conductivity, diverse microstructures, low density, and high environmental stability[11-13]. Incorporating magnetic components into carbon-based materials can introduce a dielectric-magnetic coupling effect, which helps optimize impedance matching behaviors and enhance attenuation capacity to some extent, providing a feasible strategy for designing high-performance carbon-based MAMs[14-16]. However, achieving such performance typically requires a high filler loading to establish interconnected EM response networks within a wave-transparent matrix, which often leads to processing challenges and increased costs in practical applications. Introducing porous microstructures has been proposed as an effective way to alleviate nanomaterial agglomeration and improve impedance matching.

Carbon-based aerogels with three-dimensional (3D) interconnected conductive networks and highly porous architectures can effectively address the limitations mentioned above. They achieve this by exerting dielectric-magnetic coupling derived from the carbon framework and the incorporated magnetic components. In addition, they prolong the propagation pathway of incident EM waves and promote multiple reflections and scattering due to the high specific surface area and porous microstructure[17-19]. More importantly, the microstructure of aerogels can be precisely tailored through various synthesis methods, facilitating the development of high-performance MAMs with tunable absorbing frequency bands and multifunctional integration, presenting carbon-based aerogels as significantly promising candidates for next-generation microwave absorption applications[20-24].

Carbon-based microwave-absorbing aerogel materials have emerged as a prominent research focus in recent years. Analysis of the Web of Science database reveals a consistent upward trend in carbon-based MAM research, growing from 23.98% to 30.50% over the past five years, reaching 1,766 publications in 2025. In contrast, the carbon-based aerogels account for approximately 60% of publications in the microwave absorption aerogel field [Figure 1]. The research hotspot on carbon-based microwave-absorbing aerogels has gradually evolved from the straightforward incorporation of heterogeneous components toward the rational construction of specific microstructure with different defective, interfacial, and pore properties across micro- to macro- scales, along with facilitating the synergistic effects of multiple energy absorption and dissipation mechanisms. Recent review articles have systematically introduced the role of heterogeneous components integration on carbon-based MAMs in promoting the magnet-dielectric coupling effects. Besides, the

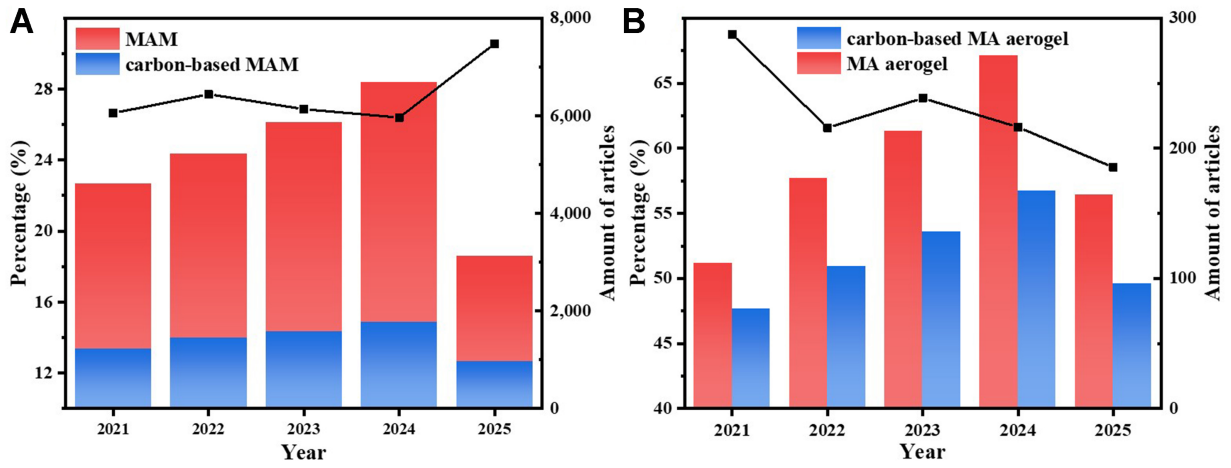

Figure 1. Schematic representation of the rapidly growing area of (A) carbon-based MAM and (B) carbon-based MA aerogel. MAM: Microwave-absorbing material; MA: microwave-absorbing.

heteroatom doping and nanoparticle confinement strategies have also been discussed to demonstrate the relationship between the defective and interfacial structures and the corresponding dielectric loss behaviors[25,26]. Compared to the reviews as mentioned above, this review systematically summarizes the advancement in carbon-based microwave-absorbing aerogels over the past five years, primarily emphasizing on the construction of 3D carbon-based aerogels with interconnected conductive networks and porous microstructure, along with revealing the significant relationship between the structure and the dielectric loss mechanisms, thereby providing research guidance for designing and constructing carbon-based aerogels to enhance the overall microwave absorption performance. At first, the EM parameters and microwave absorption mechanisms of aerogel materials are introduced, accompanied by the commonly employed testing methodologies. Subsequently, the effects of composition and microstructure on the EM response behaviors and microwave-absorbing properties of carbon-based aerogels are comprehensively analyzed, along with an in-depth discussion of recent developments categorized by synthesis methods, including hard-template, self-assembly, and other novel approaches. Finally, key challenges and future research directions for carbon-based microwave-absorbing aerogels are outlined. This review aims to provide significant references and valuable insights for the future development and potential applications of carbon-based microwave-absorbing aerogel materials with enhanced overall performance.

MICROWAVE ABSORPTION MECHANISMS

The environmental microwaves interact with MAMs in three primary ways: reflection at the material surface, absorption within the MAM, and transmission through the MAM[27-29]. The incident power can also be divided into three parts: reflection power (P_r), absorption power (P_a), and transmission power (P_t), as shown in Figure 2A. According to the energy conservation law, the propagation behavior of microwaves involves the conversion and dissipation of EM energy[30]. Therefore, an ideal MAM should allow microwaves to enter the aerogel with minimal reflection and ensure their dissipation within the internal structure rather than transmission out of the aerogel, which requires key characteristics of impedance matching behavior and attenuation capacity. Besides, dielectric and magnetic losses are the main mechanisms for absorbing microwaves in the GHz frequency band[31-33].

Dielectric loss

Dielectric loss refers to the energy loss generated by the conversion and dissipation of electric field energy in the medium during the propagation of microwave[34-36], mainly including conduction loss, dipolar

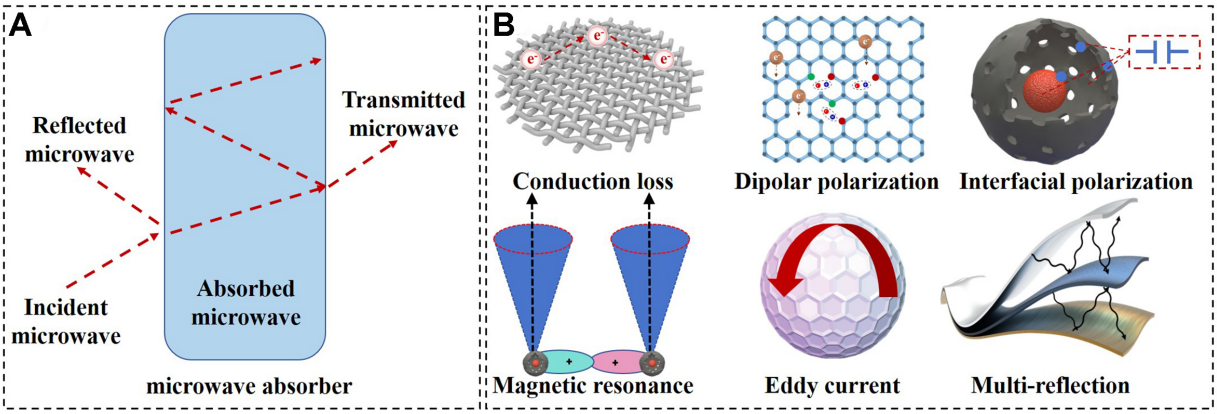

Figure 2. Schematic diagram of (A) the interaction between microwaves and MAMs; (B) Dielectric loss and magnetic loss mechanisms[38-40]. Reproduced with permission[38]. Copyright 2022, ELSEVIER. Reproduced with permission[40]. Copyright 2022, ELSEVIER. Reproduced with permission[39]. Copyright 2024, ELSEVIER. MAMs: Microwave-absorbing materials.

polarization loss, and interface polarization loss. It can be quantitatively estimated using the dielectric loss tangent (tanδe), where ε′ and ε″ represent the real part and the imaginary part of the complex permittivity ε_r. According to Debye theory, the relatively complex permittivity imaginary part (ε″) could be divided into conduction loss (ε_c'') and polarization loss (ε_p''), as given in:

$$\varepsilon_r = \varepsilon' - j\varepsilon'' \tag{1}$$

$$\tan\delta e = \varepsilon''/\varepsilon' \tag{2}$$

$$\varepsilon'' = \frac{\omega\tau(\varepsilon_s - \varepsilon_\infty)}{1+\omega^2\tau^2} + \frac{\sigma}{\omega\varepsilon_0} = \varepsilon_p'' + \varepsilon_c'' \tag{3}$$

$$\varepsilon_c'' = \frac{\sigma}{\omega\varepsilon_0} \tag{4}$$

where ω is angular frequency, ε_s is static dielectric constant, τ is polarization relaxation time, ε_∞ is relative permittivity at high frequency, and σ is electrical conductivity. The conduction loss originates from the electron hopping and migration properties of the carbon-based aerogel[37], which is positively associated with the electrical conductivity, as exhibited in Figure 2B[38-40]. As for polarization loss, it can be mainly separated into dipolar and interfacial polarization in the GHz region, while electronic and ionic polarization contribute to dielectric loss in a higher frequency range[41]. The defective sites, heteroatoms, and functional groups are usually regarded as active centers, which induce bound charge pairs, undergoing orientation and alignment under an alternating EM field. Since the direction change of the dipole pairs lags behind that of the external EM field, the repeated hysteretic rotation behaviors of the dipoles lead to the Debye relaxation effect, thereby consuming the EM energy and converting it into heat[42]. Besides, the interface polarization occurs at the interface between the hetero-components with different EM properties. The uneven distribution of space charges would accumulate on both sides of the interface under an applied electric field, fail to migrate across the interface, forming a space charge layer as a micro-capacitor microstructure, thereby converting and dissipating the EM energy effectively[43-45].

Magnetic loss

Magnetic loss refers to the magnetic interaction and the energy conversion between the MAM and the incident microwave. It is highly dependent on the magnetic components in MAMs, evaluated by the magnetic loss tangent (tanδμ), including the real part (μ′) and the imaginary part (μ″) of the complex

permeability μ_r[46]. The magnetic loss mechanisms mainly include resonance behaviors (natural, exchange, and domain), magnetic hysteresis, and eddy current effect[47]. The domain wall resonance commonly generates at MHz frequency region and magnetic hysteresis represents irreversible magnetization behaviors at higher magnetic field, which could be neglected at the GHz frequency range. The natural resonance behavior is influenced by the anisotropy and magnetic moment of the magnetic component within a single domain[48], whereas exchange resonance, occurring in exchange-coupled spin systems, is negatively correlated with the size of the magnetic particles and appears at higher frequency regions. Therefore, the magnetic loss behavior can be tailored by controlling the magnetic anisotropy of particles with different morphologies and crystalline structures[49]. Besides, eddy currents also play a crucial role in converting the microwave energy into thermal energy due to the Joule heat effect, by generating an induced micro-current under alternating EM fields[50-52], which could be evaluated as follows:

$$\mu_r = \mu' - j\mu'' \tag{5}$$

$$\tan\delta\mu = \mu''/\mu' \tag{6}$$

$$C_0 = \mu''\mu'^{-2}f^{-1} = \frac{2}{3}\pi\mu_0\sigma d^2 \tag{7}$$

where μ_0, f, σ, and d represent the vacuum permeability, frequency, conductivity, and thickness of the MAM, respectively. If the value of C_0 remains constant, the eddy current effect reflects the primary mechanism influencing magnetic loss. However, under the extremely high frequency of the external magnetic field with low resistivity of the MAM, the induced magnetic field on the surface of the material would decrease the magnetic flux density in a limited depth, leading to impedance mismatch behavior from the so-called skin effect[53-55]. Therefore, the conductivity and thickness of the material are usually adjusted to weaken the negative effect of eddy currents.

Impedance matching

The impedance matching factor Z of the material can be calculated by[56-58]:

$$Z = |Z_{in}/Z_0| \tag{8}$$

$$Z_{in} = Z_0\sqrt{\frac{\mu_r}{\varepsilon_r}}tanh[j(\frac{2\pi fd}{c})\sqrt{\mu_r\varepsilon_r}] \tag{9}$$

where Z_{in} represents the normalized input impedance of the MAM, and Z_0 is the free-space impedance with a magnitude of 377 Ω. In addition, c refers to the velocity of microwaves. If the impedance value of the external free space is equal to the impedance of the MAM, the microwave can enter the material rather than being reflected.

Attenuation capacity

As mentioned earlier, good impedance matching behavior ensures the penetration of the external microwave into the aerogel, which is the prerequisite for absorbing microwaves[59]. After that, the incident microwave is required to be attenuated efficiently. The attenuation constant α can be adopted to quantify the dissipation capacity of the MAM[60-62], as given in:

$$\begin{aligned}\alpha &= \frac{\sqrt{2}\pi f}{c} \times \sqrt{(\mu''\varepsilon'' - \mu'\varepsilon') + \sqrt{(\mu''\varepsilon'' - \mu'\varepsilon')^2 + (\mu'\varepsilon'' + \mu''\varepsilon')^2}} \\ &= \frac{\sqrt{2\mu'\varepsilon'}\pi f}{c} \times \sqrt{(\tan\delta_\mu \tan\delta_\varepsilon - 1) + \sqrt{\tan^2\delta_\mu \tan^2\delta_\varepsilon + \tan^2\delta_\varepsilon + \tan^2\delta_\mu + 1}}\end{aligned} \tag{10}$$

A larger α value indicates a stronger attenuation capability for incident microwaves, thereby dissipating EM energy and minimizing the transmission of residual waves out of the MAM.

RL

Both the optimal impedance matching and attenuation capability determine the microwave absorption performance of the aerogel, which is quantified by the RL calculated as follows[63-65]:

$$RL = 20\log_{10}\left|\frac{Z_{in} - Z_0}{Z_{in} + Z_0}\right| \tag{11}$$

If the value of the RL is less than -10 dB, more than 90% of the incident microwave can be effectively absorbed, basically meeting the requirements in practical application[66]. Besides, the EAB is defined as the frequency region where the RL value is less than -10 dB. The RL and EAB are the most critical indicators to evaluate the microwave absorption performance. Additionally, beyond the dissipation mechanisms previously discussed, the interconnected conductive networks and porous microstructures of carbon-based aerogels enhance energy consumption through multi-reflection and scattering[67,68].

Role of the aerogel in microwave absorption performance

Apart from reducing density and enabling lightweight properties, the 3D microstructure of carbon-based aerogels plays a significant role in enhancing microwave absorption performance, distinguishing them from low-dimensional carbon-based counterparts[69].

For example, Qiao *et al.* prepared porous carbon aerogels with the decoration of the highly dispersed magnetic nanoparticles[70]. The introduction of CoFe alloy nano-capsules would reduce the complex permittivity, while the complex permeability increased with the content of CoFe alloy nanoparticle within the carbon-based aerogel. More importantly, the construction of the anisotropic cellular structure plays a crucial role in influencing the EM response behaviors compared to the irregular microstructures prepared by the common mechanical mixing strategy, obtaining the optimal RL intensity of -70.8 dB and EAB of 6.0 GHz with a low filler ratio of 2.2 wt%. The contribution of aerogel toward the microwave response behaviors could be mainly described as follows[36]:

(a) The porous structure allows more air to be accommodated within the interior of the aerogel, effectively reducing the impedance mismatch between the MA aerogel and free space, thereby improving impedance matching and ensuring microwave penetration. Accordingly, the effective permittivity of the aerogel can be expressed using the Maxwell-Garnett (MG) equation, as given below:

$$\varepsilon_{eff}^{MG} = \left[\frac{(\varepsilon_2 + 2\varepsilon_1) + 2f_r(\varepsilon_2 - \varepsilon_1)}{(\varepsilon_2 + 2\varepsilon_1) - f_r(\varepsilon_2 - \varepsilon_1)}\right]\varepsilon_1 \tag{12}$$

where ε_{eff} is the theoretical effective dielectric constant, ε_1 and ε_2 are the dielectric constants of the solid and air ($\varepsilon_2 \approx 1$), respectively, and f_r represents the volume proportion of pores in the materials. The carbon-based aerogel can be regarded as a composite consisting of a solid component (carbon framework) and an air component (pore), which can reduce the effective dielectric constant and alleviate the impedance mismatching behaviors. Moreover, based on this equation, it is implied that the dielectric loss could be regulated by controlling the porosity of the aerogel.

(b) The porous structure extends propagation paths and alters propagation direction of the incident microwave, which greatly increases the contact between the microwave and the pore walls within the aerogel, promoting the energy dissipation and transforming it into heat by the multi-reflection/scattering effect.

(c) The dielectric loss effects could be improved by the unique microstructure of the aerogel. The porous structure possesses abundant carbon-air interface areas, where a significant amount of charge accumulates on both sides of the heterointerface, promoting interfacial polarization loss behaviors. Besides, the 3D interconnected conductive network skeleton of the aerogel could effectively support the transport of the electrical carriers, thereby enhancing the conduction loss.

MICROWAVE ABSORPTION PERFORMANCE OF CARBON-BASED AEROGEL BY DIFFERENT SYNTHESIS STRATEGIES

Hard-templates methods

Natural porous template

Research on natural materials has attracted widespread attention for bio-derived carbon-based microwave absorption aerogels, owing to their inherent biological tissue and porous structures, as well as eco-friendly properties such as abundant resources, diverse forms, and low cost. Many natural biomasses possess unique biological tissue structures, which can be well preserved during high-temperature pyrolysis, thus providing a facile and convenient method to construct 3D porous carbon aerogels[71]. Typically, natural woods with cellular parenchyma tissues and porous bundles are well-recognized precursors for carbon-based microwave-absorbing aerogels, but they exhibit unsatisfactory microwave-absorbing performance due to relying solely on the dielectric loss mechanism. Incorporating magnetic components is widely adopted to tailor the EM response characteristics and the corresponding MA performance effectively[72].

Zhao *et al.* prepared magnetic nickel-decorated carbon aerogel composites via a direct impregnation approach, using $NiCl_2$ and poplar wood as raw materials[73]. The wood matrix was immersed in a hydrated nickel chloride solution and subjected to vacuum impregnation. Following complete drying, high-temperature carbonization was performed at different temperatures to prepare target composites, which directly influenced the microwave absorption characteristics. When the carbonization temperature was set to 700 °C, the minimum RL value reached -60.4 dB at a thickness of 2.93 mm. Furthermore, the EAB was greatly extended to 7.3 GHz at a thickness of 2.63 mm. To address weak interfacial bonding and uneven component distribution from the direct immersion method, Gou *et al. in situ* grew bimetallic organic frameworks on balsa wood via co-precipitation, followed by high-temperature annealing under a protective atmosphere to obtain CoNi-modified wood-derived carbon composites[74]. When the pyrolysis temperature was 700 °C, the optimal RL value reached -25.96 dB at 17.98 GHz with a thickness of 1.8 mm.

In addition to the co-precipitation method, hydrothermal and solvothermal methods are also considered feasible approaches for constructing bio-derived porous MAM. Cui *et al.* successfully prepared high-performance magnetic component-loaded porous carbon composites using wood as raw material through hydrothermal and carbonization processes[75]. The uniform distribution of magnetic nanocomposites maintained the porous microstructure of the carbon framework and contributed to multiple EM dissipation mechanisms, thereby achieving outstanding microwave absorption performance with the RL of -62.235 dB at a thickness of just 2.42 mm. Cui *et al.* employed a porous structure engineering strategy to fabricate a high-performance Co/niobium carbide (Nb_2CT_x)/carbon aerogel composite material[76]. Compared with bamboo cellulose carbon aerogels, the introduction of conductive Nb_2CT_x and the magnetic Co component could effectively improve the impedance matching behaviors of the corresponding Co/Nb_2CT_x/carbon aerogel. Besides, the 3D interconnected network heterostructure not only promoted conduction loss but also facilitated the multi-reflection and multi-scattering effects, thereby exhibiting a remarkable RL value of -60.25 dB at a thickness of 1.67 mm and a low density of 54.03 mg·cm^{-3}. Furthermore, the Radar Cross Section (RCS) simulation results indicate the aerogel's effectiveness in reducing its detectability.

Besides, Shen *et al.* synthesized balsa wood-derived carbon aerogels loaded with magnetic metals via a solvothermal method, followed by high-temperature carbonization[77]. The pore structure of the wood-based substrate exerted a regulatory effect on the reflection and scattering of EM waves, while the incorporation of magnetic fillers optimized impedance matching. This synergistic design enhanced both dielectric and magnetic loss mechanisms, thereby obtaining improved microwave-absorbing performance.

In addition to introducing magnetic components into carbon-based aerogels to enhance performance by supplying magnetic loss, doping heteroatoms into the carbon-based framework is another commonly used method to effectively tailor dielectric loss and thereby improve microwave absorption performance. Xiao *et al.* used fir wood as a raw material to *in situ* grow nitrogen-doped carbon nanotubes (CNTs) within wood-derived porous carbon, while simultaneously loading magnetic cobalt nanoparticles[78]. The composites exhibited a 3D conductive network structure with excellent impedance matching behavior, in which both polarization loss and conduction loss could be tailored during the doping process, thereby demonstrating controllable microwave absorption performance. Besides, cotton[79], bamboo[80], and loofah sponge[81] can serve as substrate materials to prepare lightweight biomass-derived carbon aerogels. Their natural hierarchical porous microstructures provide abundant adsorption sites for metallic ions, which can be *in situ* converted and reduced to various magnetic components during calcination, resulting in higher RL values and broader EAB.

Polymer foams template

In addition to natural biomass with unique 3D structures, polymers with 3D porous structures are also regarded as ideal templates for preparing corresponding carbon-based aerogels with different components, while maintaining the pore structure effectively.

Li *et al.* prepared nitrogen-doped CNTs and CoO/Co nanoparticle-modified carbon aerogels by pyrolyzing a zeolitic imidazolate framework (ZIF)-decorated melamine foam template[82]. The magnetic particles contributed to magnetic losses and effectively optimized impedance matching, while heteroatom doping enhanced dipolar polarization. In addition, the unique porous nanotube structure promoted multi-reflection and multi-scattering of incident microwaves, achieving a minimum RL value of -52.3 dB. Yu *et al.* synthesized magnetic nitrogen-doped porous carbon-based MAM using melamine foam as a template[83]. By adjusting the heat treatment temperature, both the microstructure and EM response could be controlled. The ultralight aerogel could be supported on Setaria viridis, achieving a minimum RL value of -44.15 dB at 11.18 GHz with a thickness of 2.5 mm, attributed to the synergistic effect of hetero-components and the porous microstructure. In addition to individually loading particles and CNTs on 3D porous melamine foam templates, Yu *et al.* successfully prepared zero-dimensional (0D) magnetic particles, one-dimensional (1D) CNTs, and two-dimensional (2D) MXene-loaded 3D porous carbon-based composites via surface treatment, self-assembly, and *in situ* growth strategies[84]. The results demonstrated that the melamine-derived composites possessed an effective microwave absorption bandwidth of 4.72 GHz, providing new insights for the development of carbon-based porous MAMs with coexisting multidimensional components. Similarly, Jia *et al.* synthesized the carbon-based porous microstructure with the decoration of the magnetic nanoparticles and the CNTs through chemical vapor deposition methods[85]. By altering the deposition time to regulate the composition, both the EM parameters and the corresponding microwave absorption performance of the sample could be controlled. When the pyrolysis time of C_2H_2 was 60 min, the microwave absorber exhibited a strong absorption capacity of -44.48 dB, a wide effective absorption frequency range of 5.0 GHz, a thin matching thickness of 1.68 mm, and a low density. Furthermore, magnetic nanoparticles-encapsulated CNTs can be *in situ* grown on carbonized melamine foam via a facile carbonization method[86], as shown in Figure 3. The magnetic-dielectric coupling effect could be enhanced by tailoring the concentration of the precursor, thereby optimizing the RL value to -75.4 dB at 5.2 GHz.

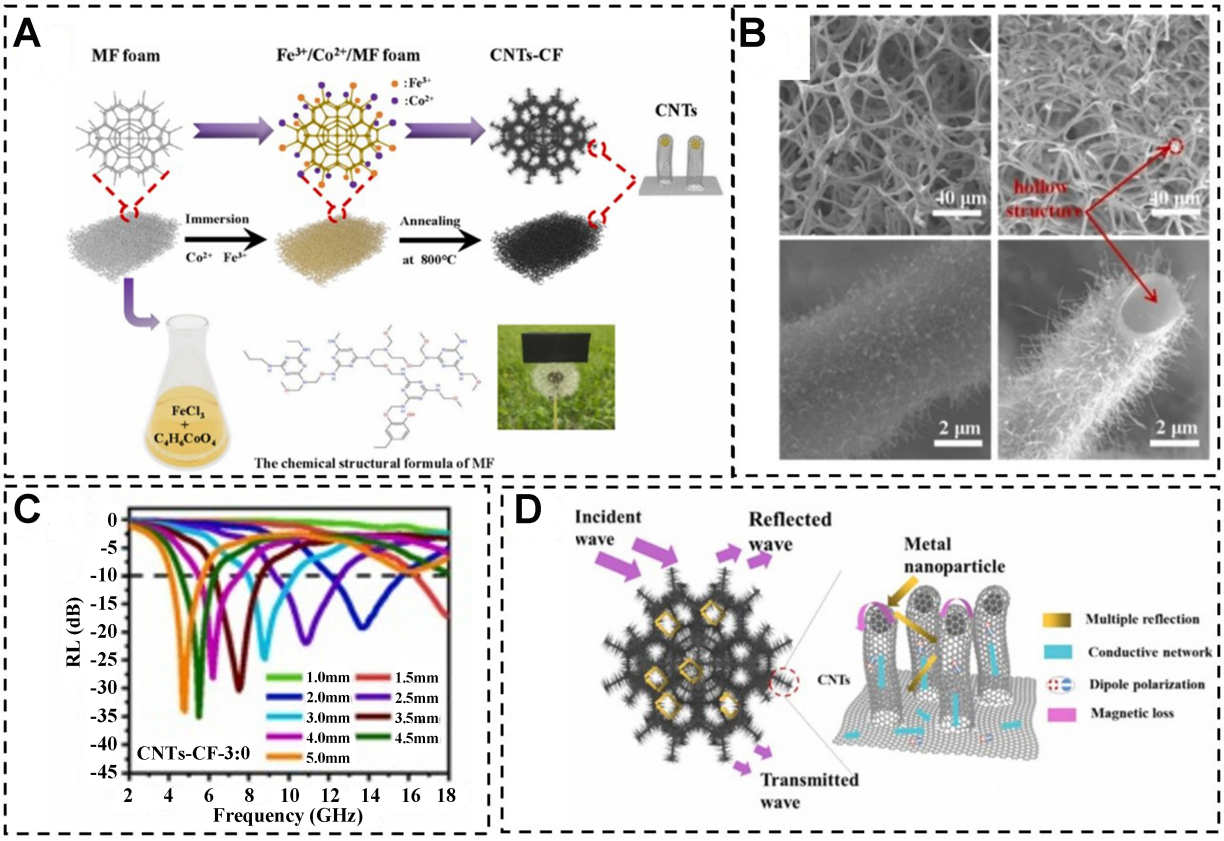

Figure 3. (A) Schematic of the preparation process, (B) microstructure, (C) RL properties, and (D) microwave absorption mechanism of CNTs-CF[86]. Reproduced with permission[86]. Copyright 2023, ELSEVIER. RL: Reflection loss; CNTs-CF: carbon nanotubes-carbon foam; MF: melamine foam.

In addition to melamine foam, polyurethane[87] and phenolic resins[88] have also been used as hard templates for constructing carbon-based porous materials decorated with hetero-components via hydrothermal and thermal treatments. A comparison of the microwave absorption performance of carbon-based aerogels prepared by hard-template methods is presented in Table 1. In summary, hard-template methods can successfully produce porous carbon-based MAM with inherent hierarchical structures and tailored components, enabling convenient regulation of EM response characteristics.

Soft-template methods

Although research on carbon-based aerogels prepared from 3D templates has made significant progress in microwave absorption, the fixed porous structure and the surface modification limit the wide-range regulation of the EM response behaviors. Adopting the soft-template method is an effective strategy to address the above issue.

Freeze-drying strategy

Freeze-drying is the most employed soft-template method. During the freezing process, as ice crystals grow, the components in the suspension are concentrated and confined in the spaces between them, forming a solid skeletal structure templated by the ice. Subsequently, under low-temperature and high-vacuum conditions, the ice crystals sublimate directly into vapor, leaving a porous structure that replicates the spaces previously occupied by the ice, resulting in an aerogel with high porosity.

Table 1. Comparison of microwave absorption performance of carbon-based aerogels with the hard-template method

Sample	Mass ratio (%)	Optimal RL (dB)	*f* at optimal RL (GHz)	d (mm)	EAB (GHz)	Ref.
WPC_{700}-Ni	20	-60.40	~15.00	2.93	7.30	[73]
WNC-700	30	-25.96	17.98	1.80	-4.10	[74]
$NiFe_2O_4/Ni_3Fe$@MC	10	-62.26	~6.00	2.42	6.72	[75]
Co/Nb_2CT_x/carbon	10	-60.25	~16.00	1.67	4.00	[76]
Co@WCA	-	-70.40	~10.00	2.40	3.30	[77]
Fir@Co@CNT	20	-52.00	10.72	2.30	4.20	[78]
CN-2.5	20	-53.00	~4.00	1.65	5.08	[79]
MDBC-8		-47.06	7.76	2.75	2.80	[80]
carbon/Fe_3O_4	50	-52.54	~7.00	4.50	5.28	[81]
CoO/Co/N-CNTs	20	-52.30	14.24	2.00	5.28	[82]
MFNC-700	25	-44.15	11.18	2.50	5.30	[83]
MFTC-900	-	-24.83	~16.00	1.30	4.72	[84]
CF/CNTs@Fe_3C@Fe_3O_4	30	-44.48	16.00	1.68	5.00	[85]
CNTs-CF	10	-75.40	5.20	4.63	-	[86]
PM-700	28	-54.70	17.28	1.40	6.40	[87]
MCF-2	15	-54.02	8.92	3.05	8.92	[88]

RL: Reflection loss; EAB: effective absorption bandwidth; CNT: carbon nanotube.

Isotropic freeze-drying strategy

The isotropic freeze-drying technology holds broad application prospects and significant potential due to its operational simplicity and minimal raw material constraints. The preparation of 3D porous carbon-based aerogels from abundant biomass extracts using freeze-drying technology carries substantial economic and environmental significance. Natural biomass extracts are essentially high-molecular-weight polymers, enabling the regulation of carbon-based aerogel composition and structure to enhance their microwave absorption capability. Cellulose is the most abundant natural polymer and can be obtained from a variety of plants, including wood, bamboo, cotton, reeds, nutshells, and fruit peels, making it a preferred precursor for preparing carbon-based aerogels.

Shao *et al.* synthesized ultralight covalent organic framework/graphene (COFG) Schottky-heterojunction aerogels via simple assembly and freeze-drying routes [Figure 4][89]. By changing the thickness and coverage of the covalent organic framework nanolayer, the polarization and conduction losses could be effectively tailored. Furthermore, benefiting from the abundant heterogeneous interfaces, the aerogels exhibited outstanding microwave absorption properties, with an optimal RL value of -79.8 dB at 6.12 GHz and a wide EAB of 6.96 GHz at a thickness of 2.35 mm. Similarly, Guo *et al.* synthesized cellulose-based carbon aerogels modified with magnetic FeCo alloy nanoparticles via hydrothermal synthesis, freeze-drying, and high-temperature pyrolysis[90]. The hydrothermal method effectively ensured uniform dispersion of calcined magnetic FeCo alloy nanoparticles, facilitating optimal impedance matching and enhanced magnetic and dielectric losses. Furthermore, the porous structure of the aerogel induced multiple reflection/scattering effects, further attenuating incident microwaves. It exhibited a minimum RL value of -49.5 dB at 9.84 GHz and a maximum EAB of 10.88 GHz, covering the entire Ku-band and X-band frequency regions.

The heterojunctions offer significant advantages in tailoring EM response behaviors. Incorporation of magnetic components can induce magnetic resonance and modulate interfacial polarization, effectively

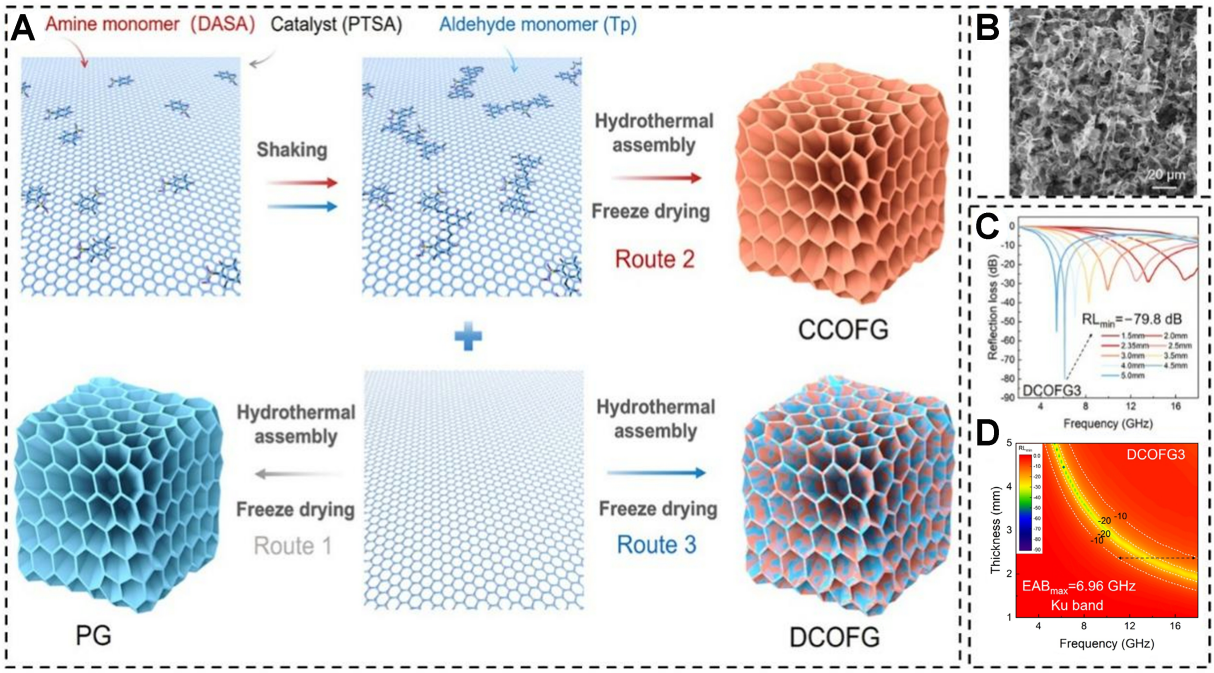

Figure 4. (A) Scheme of the synthetic procedure, (B) SEM image, and (C and D) RL behaviors of DCOFG3 hetero-structured aerogel[89]. Reproduced with permission[89]. Copyright 2025, WILEY-VCH. SEM: Scanning electron microscope; RL: reflection loss; PG: porous RGO; CCOFG: continuous COF-confined RGO; DCOFG: discrete COF-confined RGO; EAB: effective absorption bandwidth; RL_{min}: minimal value of Reflection loss.

facilitating magnetic-dielectric coupling. In addition, heteroatom doping is an effective strategy to adjust the conductivity of the carbon-based framework, generating dipolar pairs due to the electronegativity difference between the dopants and carbon atoms. These dipoles promote polarization under an external alternating EM field with relaxation behavior, thereby enhancing the polarization loss of the carbon-based MA aerogel[91].

Zhu *et al.* focused on the multicomponent and heterogeneous structures of cellulose aerogels, preparing nitrogen-doped cellulose-derived carbon-based aerogels (CCMC/ZnO@Ni)[92]. This multidimensional structural configuration enabled tunable EM properties and excellent impedance matching behaviors when compared to the carboxymethyl cellulose aerogel and ZnO@Ni aerogel counterparts. Notably, Schottky contacts at heterogeneous interfaces induced strong interfacial polarization effects, improving the MA performance. Density functional theory calculations further revealed that the unique Schottky barrier caused band bending, promoting directional electronic migration at interfaces and generating internal electric fields. This significantly accelerated multiple relaxation processes in the resulting carbon-based aerogel, yielding an enhanced RL of -64.0 dB at 13.9 GHz and an EAB of 4.9 GHz with a thickness of 2.0 mm. Wang *et al.* prepared nitrogen-doped magnetic carbon-based aerogels containing nanofibers and aligned Ni chains via freeze-drying followed by annealing[93]. Notably, the composite exhibited outstanding MA performance, achieving a minimum RL of -62.0 dB and a wide EAB covering the Ku band (12.4-18.0 GHz) completely. The outstanding MA performance originates from a 1D/2D/3D-supported interpenetrating network structure, which exhibited eye-catching impedance matching, dielectric loss, magnetic loss, interfacial polarization, dipolar polarization, multiple reflection and scattering characteristics. Su *et al.* enhanced microwave absorption by embedding multilayer hollow cobalt sulfide into heteroatom sulfur-doped carbon aerogels[94]. The formation of the hollow structure and the point defects could be controlled from the migration of the sulfur atoms via the Kirkendall effect, which significantly enhanced the RL value to -52.82 dB and a broader

EAB of 8.82 GHz. Additionally, the first-principles calculations and far-field simulations comprehensively validated the contribution of the hetero-atom doping to the microwave absorption performance.

The natural biomass materials, such as chitosan[95], sodium alginate[96,97], gelatin[98,99], and carrageenan[100], are commonly used as carbon-based precursors for preparing 3D carbon aerogels due to their wide availability from natural sources, including shrimp, crabs, insects, and mollusks. Chitosan's molecular chains are rich in amino groups, providing exceptional metal ion capture capabilities and enabling the formation of magnetic carbon-based aerogels. Similarly, the remarkable biocompatibility of sodium alginate, an environmentally friendly carbohydrate extracted from seaweed, allows the formation of a stable gel network upon cross-linking with metal ions, making it an ideal precursor for synthesizing interconnected carbon frameworks. In addition, the nitrogen present in these biomolecules facilitates effective heteroatom nitrogen doping in the carbon framework, thereby enhancing dielectric loss.

Luo *et al.* grew 0D magnetic cobalt nanoparticles onto a chitosan-derived nitrogen-doped carbon framework via a simple liquid reaction, freeze-drying, and calcination process[101]. The resulting Co/C aerogel exhibited a dielectrically and magnetically coupled network under optimal cobalt content conditions, achieving a minimum RL of -44.70 dB at a thin thickness of 1.35 mm and a maximum EAB of 5.45 GHz at a thickness of only 1.5 mm. Peng *et al.* synthesized lightweight porous Fe_3O_4-Fe/carbon aerogels (FFCA) by depositing magnetic metals onto a chitosan-reinforced carboxymethyl cellulose matrix with different carbonization temperatures[102]. The 3D porous structure and non-homogeneous interconnected conductive framework endowed the carbon-based aerogel with outstanding characteristics. Specifically, the incorporation of magnetic materials and carbonization at gradient temperatures enabled tunable EM parameters and excellent impedance matching. The resulting FFCA-900 aerogel exhibited outstanding RL intensity of -45.5 dB at 2.6 mm and an EAB of 3.7 GHz. Guo *et al.* successfully constructed carbon-based aerogels by *in situ* growth of CNTs via chemical vapor deposition and freeze-drying, effectively enhancing polarization relaxation and optimizing impedance matching, achieving a remarkable RL of -51.6 dB and a wide EAB of 5.9 GHz[103].

Carbon materials with sp^2 graphitized structure, such as graphene[104] and CNTs[105], are commonly used as raw materials for constructing aerogels due to their intrinsic electrical conductivity and abundant functional groups. Wang *et al.* prepared the reduced graphene oxide (RGO)-based composite aerogel modified by nickel nanoparticles from different contents of graphene oxide (GO) nanosheets and nickel-based metal-organic frameworks after freeze-drying and high-temperature pyrolysis, which exhibited high porosity and low density[106]. When the content of GO nanosheets was rationally regulated, both the pore structure and the dielectric loss properties could be tailored, which can effectively enhance the overall dissipating capability of RGO-based aerogel, thereby broadening the EAB to 5.2 GHz with a promising thickness of 1.5 mm. Besides, Shu *et al.* prepared 3D porous Co and CoO-loaded RGO aerogels by freeze-drying and high-temperature reduction techniques[107]. By controlling the pore structure, EM parameters could be effectively adjusted, achieving the minimum RL value and EAB of -61.8 dB and 4.2 GHz, respectively.

Directional freeze-drying strategy

The conventional freeze-casting method typically involves the solidification of a carbon-containing solution in a uniformly low-temperature environment. Owing to isotropic ice nucleation and an uncontrolled crystallization process, both the orientation and the morphology of the resulting ice crystals are difficult to control, leading to a disordered and unpredictable porous microstructure. In contrast, directional freezing strategy enables the construction of highly ordered pore architectures through the templating effect of unidirectionally growing ice crystals under a controllable thermal gradient, which facilitates the rational design of aligned porous frameworks in carbon-based aerogels with tunable EM response characteristics effectively[108].

Specifically, by placing the bottom of the carbon-based solution container on a cold source and maintaining a relatively higher temperature at the top, a stable and directional thermal gradient is established across the sample. The ice crystals would nucleate near the cold interface and grow directionally toward the warmer region, excluding and confining the carbon-based components between the gaps of the adjacent lamellar ice crystal array, obtaining carbon-based aerogel with a highly ordered, anisotropic, and layered porous structure after removing the ice template by sublimation treatment. Moreover, by tuning the key processing parameters[109], such as the thermal gradient and freezing rate, the pore size, wall thickness, orientation and direction of pores can be tailored, enabling the construction of a hierarchically aligned structure spanning from the micro- to macro-scale. The resulting anisotropic porous architecture produced by directional freezing methods significantly influences the microwave propagation behaviors. Incident microwaves undergo multiple internal reflections and scattering at channel walls and heterogeneous interfaces, rather than penetrating the aerogel directly. This significantly prolongs their propagation path within the aerogel, increasing opportunities for EM energy dissipation.

Fei *et al.* prepared carbon-based aerogels by growing cobalt nanoparticles on CNTs within a conductive framework via directional freeze-casting followed by carbonization[110]. Owing to the unique 3D porous structure with a large surface area, abundant interfacial defects, and efficient electrical conductivity, the resulting carbon aerogel exhibited a minimum RL of -27.5 dB and an excellent EAB of 7.4 GHz. Li *et al.* prepared honeycomb-like anisotropic porous channels via unidirectional freeze-drying of a chitin nanofiber/water suspension, while the carbon-based defective microstructure could be effectively tailored by controlling the carbonization temperature[111]. The resulting aerogels exhibited outstanding microwave absorption performance for microwaves applied both parallel and perpendicular to the anisotropic channels. The chitin-derived carbon aerogels were then subjected to controlled compression from 0% to 80% to investigate the corresponding EM response behaviors[112], achieving a maximum RL of -40 dB while covering the entire X-band region after 60,000 compression-recovery cycles. Furthermore, radial freezing strategies, a special type of unidirectional freezing, can produce aerogels with unique pore structures containing numerous interfaces[113,114], enhancing interfacial polarization and dielectric loss, thereby improving RL intensity and EAB.

Compared to unidirectional freezing, bidirectional freezing is more attractive for synthesizing aerogels with ordered and layered microstructures. To achieve broadband absorption, lamellar RGO-based aerogels were successfully synthesized via bidirectional freezing and subsequent thermal annealing[115], exhibiting exceptional microwave absorption with a minimum RL of -72.2 dB at a thickness of 2.1 mm and an EAB of 8.4 GHz within 9.6-18.0 GHz. Liang *et al.* constructed a Ni nanochain-anchored 3D MXene/RGO aerogel (NiMR-H) using bidirectional freezing followed by chemical reduction with hydrazine vapor [Figure 5A], forming dielectric/magnetic heterogeneous interfaces with an oriented pore structure[116]. This aerogel exhibited an enhanced RL of -75.2 dB with a wide EAB of 7.3 GHz, attributed to improved impedance matching and magnetic-electric coupling. Moreover, the RL response toward incident microwaves differed between the parallel and perpendicular directions of the anisotropic aerogel. To explore the interaction between incident microwaves and the directional macroporous structure, Du[117] measured the EM parameters at different incident angles [Figure 5B]. Both the complex permittivity and the α value decreased as the incident wave direction changed from perpendicular (90°) to parallel (0°) to the channels, while impedance matching increased, due to enhanced microwave propagation along the directional pore channels. Therefore, the pore orientation affects the trade-off between impedance matching and attenuation, leading to direction-dependent microwave absorption performance.

The gradient-structured aerogel simultaneously enhances impedance matching and microwave attenuation by engineering a heterogeneous pore structure. This structure exhibits a continuous spatial gradient in EM

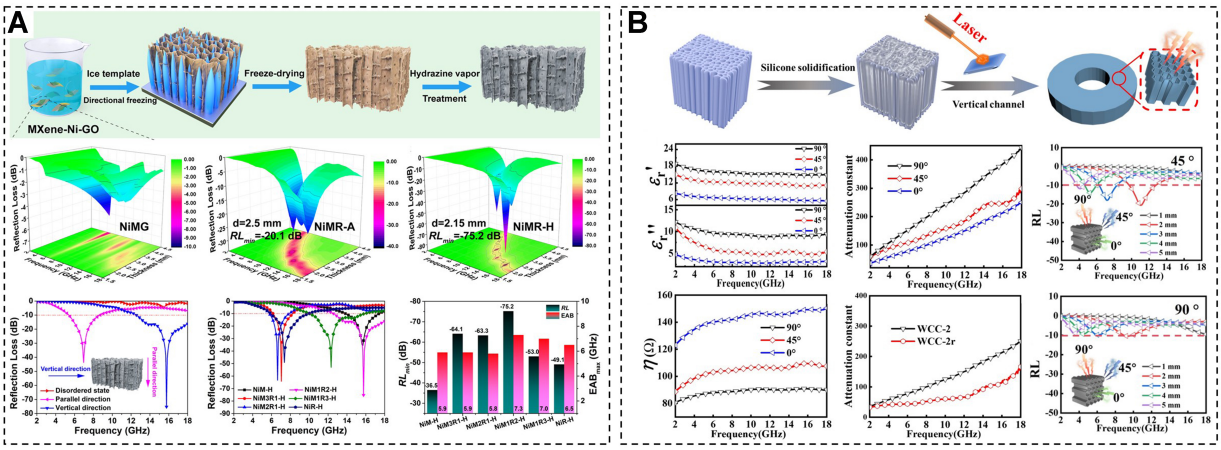

Figure 5. The construction and microwave absorption properties of (A) Ni/MXene/RGO aerogel[116] and (B) WCC foams[117] with different pore orientations. Reproduced with permission[116]. Copyright 2021, American Chemical Society. Reproduced with permission[117]. Copyright 2025, Springer Nature. WCC: Tungsten carbide carbon foam; GO: graphene oxide; RL: reflection loss; EAB: effective absorption bandwidth.

parameters from the surface to the interior, thereby enabling efficient dissipation of incident microwaves across a broad frequency range at distinct depths.

Specifically, the outermost layer of the aerogel typically exhibits a highly macroporous microstructure with an effective impedance closely matched to that of free space, which minimizes surface reflection and facilitates deeper penetration of incident microwaves into the aerogel. As the pore structure and conductive network density progressively vary across successive layers, the gradual increase in effective permittivity and permeability within the intermediate region promotes propagation and dissipation of incident microwaves via dielectric and magnetic loss. Subsequently, the microwaves reflect from the bottom of the aerogel to the middle layer, where they interfere with incoming waves of opposite phase, thereby consuming microwave energy through repeated interactions with the carbon-based framework. By constructing an "absorption-reflection-reabsorption" transmission path, the microwaves are dissipated and converted to thermal energy over an exceptionally wide frequency range, resulting in a significant enhancement of EAB compared to conventional homogeneous aerogels. In addition, computer simulation technology (CST) simulations of the electric field, magnetic field, and power loss distribution were conducted to highlight the role of the gradient structure in optimizing impedance matching and enhancing the multi-reflection effect within the aerogel[118-121].

The orientation and alignment of the porous structure also play a critical role in tailoring microwave response[122]. Conventional isotropic freeze-drying or chemical foaming methods typically produce aerogels with disordered, randomly oriented pores, which lead to limited control over microwave propagation pathways and only modest improvement in attenuation. In contrast, aerogels with vertically aligned, anisotropic pore channels offer advantages through directional templating strategies. Specifically, the aligned channels allow microwaves to penetrate the aerogel along the pore axis with minimal interfacial reflection. Moreover, the aligned pore walls promote directional reflection and scattering of microwaves within the aerogel, facilitating repeated interactions with the conductive carbon framework and thereby enhancing energy dissipation over an ultrabroad frequency range.

Other soft-templates

In addition to obtaining 3D porous structures through freeze-drying technology using ice templates, templates such as silicon dioxide (SiO_2) microspheres, polystyrene (PS) microspheres, polymethyl

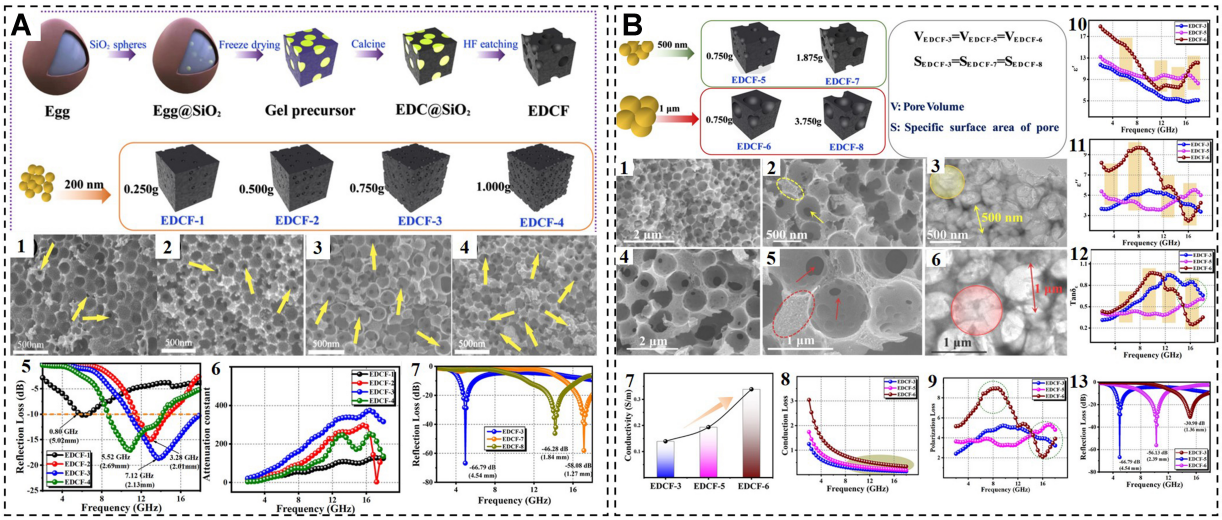

Figure 6. Schematic illustration of the synthesis process, microstructure, and the microwave absorption properties of EDCF samples with different (A) amounts and (B) diameters of silica microspheres[124]. Reproduced with permission[124]. Copyright 2022, Springer Nature. EDCF: Egg-derived porous carbon foam; HF: hydrogen fluoride.

methacrylate (PMMA) microspheres and salt crystals can also be introduced into the system to construct porous carbon-based aerogels.

SiO_2 microspheres have always been commonly used as a template to construct 3D porous structures due to their wide-range adjustable size[123]. Zhang *et al.* constructed egg-derived porous carbon foam (EDCF) MAMs using SiO_2 as a template, followed by carbonization and hydrogen fluoride (HF) etching methods [Figure 6][124]. By tailoring the amount of microspheres, both the porosity and the EM parameters of the ordered porous EDCF could be controlled, revealing the contribution of either the number or the diameter of pores in influencing the polarization loss of the incident microwave, achieving an optimal RL value of -58.08 dB with the thickness of 1.27 mm. Besides, the ultra-wide EAB of 7.12 GHz was achieved in the aerogel with smaller pore sizes.

The PMMA and PS microspheres can be directly decomposed during high-temperature treatment, which could be adopted as a soft template to synthesize aerogel materials. Xiao *et al.* used PS microspheres as templates for a two-step *in-situ* growth process, including the coating of these microspheres with Fe_3O_4, and then *in-situ* growing Fe-Co Prussian blue analogs[125]. A unique porous hollow nanostructure was generated by calcining the precursor at different temperatures. This nanostructure not only facilitated the occurrence of various interface polarizations but also promoted the multi-reflection and multi-scattering of incident EM waves, effectively. When the temperature was 600 °C, the synthesized carbon-based aerogel reached a minimum RL value of -57.01 dB and the maximum EAB of 4.58 GHz, covering almost the entire X band. Chen *et al.* used PMMA templates to prepare 3D ordered macroporous carbon-based materials with different pore size distributions by changing the size of the spheres template, which could effectively adjust the dielectric loss and the corresponding impedance matching behaviors, thereby optimizing the RL intensity to -42.33 dB at 4.8 GHz[126].

Due to their good solubility in water, salt crystals have recently been adopted as promising templates for constructing aerogels[127-129]. Guo *et al.* reported a porous carbon-based material synthesized via a NaCl template-assisted method combined with high-temperature calcination[130]. This material demonstrated highly efficient EM wave absorption while maintaining lightweight and broadband characteristics, achieving

an exceptional RL of -71.13 dB at 13.76 GHz with a thickness of only 2.46 mm, along with a broad EAB of 7.04 GHz. Wu *et al.* constructed rich heterogeneous interfaces within a hierarchical structure through a synergistic strategy combining NaCl templates and freeze-drying, preparing carbon-based EM wave absorbers loaded with Co/$Co(OH)_2$[131]. By controlling the carbonization temperature, remarkable EM heterostructures and strong interfacial polarization effects were obtained. At a thickness of 2.2 mm, the optimal RL and EAB reached -25.8 dB and 7.1 GHz, respectively.

The pore size distribution plays a critical role in determining the impedance matching behaviors and the dielectric loss of carbon-based aerogels[132]. For example, Zhang *et al.* successfully fabricated RGO-wrapped cellulose nanofibril (CNF)/GO aerogels with a tunable pore structure[133]. By increasing polyvinyl alcohol (PVA) concentration from 0 to 15 $mg \cdot mL^{-1}$, the average pore size of the RGO@CNF/GO composite aerogels decreased from 154 to 45 μm, while the dielectric loss tangent increased correspondingly, leading to the enhancement of the microwave loss capacity. Moreover, the ε'' values varied with pore size; the RGO@CNF/GO-15 sample exhibited the highest conduction loss, which is attributed to the optimized pore size distribution and PVA content, promoting suitable permittivity with interconnected conductive networks, thereby exhibiting excellent microwave attenuation performance. Besides, Wang *et al.* reported uniform vesicle-structured carbon spheres, which show remarkable microwave absorption performance due to the existence of gradient pore size distributions[39]. First, the large pores with through-hole microstructure in the vesicle carbon spheres allow the penetration of the microwave into the interior of the aerogel by improving the impedance matching behavior. Second, the abundant mesopores with a pore size of 8 nm promoted the Debye relaxation effect due to the high specific surface area, which enhanced the interfacial polarization significantly.

Macropores with larger diameters can significantly reduce both the density of the conductive network and the effective permittivity of the aerogel, which is essential for achieving favorable impedance matching with free space, thereby minimizing surface reflection and facilitating deeper microwave penetration into the aerogel[134]. Furthermore, macropores promote multiple internal reflections and scattering by extending the propagation path of incident microwaves, enhancing energy absorption and dissipation. In addition, dielectric loss can be tailored by controlling polarization behaviors arising from mesoporous and microporous structures at the nanoscale. The high specific surface area of the mesoporous structure creates numerous heterogeneous interfaces between the conductive carbon skeleton and air voids, where charge carriers can accumulate to form micro-capacitor-like structures, facilitating relaxation behaviors and enhancing interfacial polarization. Moreover, defects in the micropore walls can act as dipolar centers that modulate local electron density without significantly altering electrical conductivity and conduction loss, generating dipole polarization under an alternating EM field and resulting in EM energy attenuation. The comparison of microwave absorption performance of carbon-based aerogels prepared via the soft-template method is shown in Table 2.

Non-template strategies

Although the previously mentioned methods for preparing carbon-based aerogels have been widely adopted, they also exhibit certain shortcomings that make them difficult to meet practical requirements in some cases. Therefore, non-template strategies with broad applicability have gradually emerged.

For example, electrospinning has attracted widespread attention in constructing MA aerogel[135,136]. Wu *et al.* prepared lightweight MXene/C aerogels via electrospinning. The combination of a 3D interconnected conductive network and heterogeneous components effectively enhanced interfacial polarization and impedance matching, endowing the aerogel with excellent microwave-absorbing properties: the minimum RL reached -53.02 dB at a thickness of 3.8 mm[137]. Additionally, the composite aerogel exhibited good

Table 2. Comparison of microwave absorption performance of carbon-based aerogels with the soft-template method

Sample	Mass ratio (%)	Optimal R_L value (dB)	*f* at optimal RL (GHz)	d (mm)	EAB (GHz)	Ref.
DCOFG3	7	-79.80	6.12	2.35	6.96	[89]
FeCo@CCA-100	20	-49.50	9.84	4.05	10.88	[90]
MTF-2	40	-46.30	4.64	4.35	2.24	[91]
CCMC/ZnO@Ni	40	-64.00	13.90	2.00	4.90	[92]
Ni/CNCA	-	-62.00	~14.20	2.00	6.00	[93]
CSC-70	1.20	-52.82	11.56	3.10	8.82	[94]
CMCA	11	-59.80	~13.80	2.68	6.37	[95]
SiCw@C-Fe	-	-49.20	10.90	2.00	3.60	[96]
P/SiC_{90}@Co-C	-	-40.08	~12.00	1.90	4.16	[97]
MNG-7	-	-36.10	~12.30	3.10	~4.20	[98]
Fe_3N@C	-	-77.60	~17.50	2.20	7.76	[99]
Co/Ni-CAs	33	-48.30	~10.00	2.30	6.76	[100]
CA-Co-1.0	25	-44.70	~17.30	1.35	5.45	[101]
FFCA-900	-	-45.50	9.40	2.60	3.70	[102]
GFC-2	6	-51.60	~11.80	2.40	5.90	[103]
NCGCA-3	15	-22.70	18.00	1.30	5.20	[106]
Co/CoO/RGO	-	-61.80	~11.90	3.80	4.20	[107]
FeO_x@C/CNTs@RGO	3	-88.70	~13.70	2.99	7.30	[108]
HPWA-2	-	-66.60	11.70	5.25	4.20	[109]
CNS/Co@NCNT-900	5	-27.50	4.60	2.50	7.40	[110]
Chitin-derived carbon	-	-92.80	11.60	6.61	4.20	[111]
Chitin-derived carbon	-	-40.00	10.40	6.90	~4.20	[112]
Carbon@RGO/Fe_3O_4	5	-61.00	13.84	2.50	6.88	[113]
FMCM	40	-51.20	11.10	2.90	4.70	[114]
ZFGA4		-72.20	~16.00	2.10	8.40	[115]
NiMR-H	0.64	-75.20	~15.80	2.15	7.30	[116]
WCC-2	-	-72.00	~12.00	2.60	6.30	[117]
FeSiB@C@$NiBr_2$	70	-59.00	9.10	3.00	7.00	[118]
PPy@BNC	-	-53.00	9.40	4.00	4.20	[119]
MC/RGO	5	-62.40	~15.00	2.20	5.70	[120]
CNF/FeCoNi/CNT10	-	-43.60	16.59	2.50	7.43	[121]
CNW/Si_3N_4	1.84	-50.21	10.80	3.00	4.20	[122]
Co-OPC-2	20	-43.19	~16.50	1.70	6.86	[123]
EDCF-7	5	-58.08	16.86	1.27	~3.00	[124]
Fe_3O_4@PBA	20	-57.01	10.20	4.00	4.58	[125]
3DOM RF-300	17	-42.33	10.72	2.40	4.80	[126]
3D-CFO@CN-2	20	-52.29	~15.50	2.00	5.36	[127]
CN-Ni-1.2	-	-43.28	~16.00	2.00	5.00	[128]
Fe_3O_4@NC-700	-	-65.50	14.50	2.30	7.10	[129]
Ni@SiO_2/NGN	15	-71.13	13.76	2.46	7.04	[130]
S-0.8-700	20	-25.80	~14.00	2.20	7.10	[131]
FP-7	30	-71.30	~14.80	1.87	4.64	[132]
RGO@CNF/GO-10	-	-47.30	~9.50	3.00	9.44	[133]
CSC-327	5.5	-36.10	17.52	1.60	6.32	[39]

RL: Reflection loss; EAB: effective absorption bandwidth; CNTs: carbon nanotubes; RGO: reduced graphene oxide; 3D: three-dimensional.

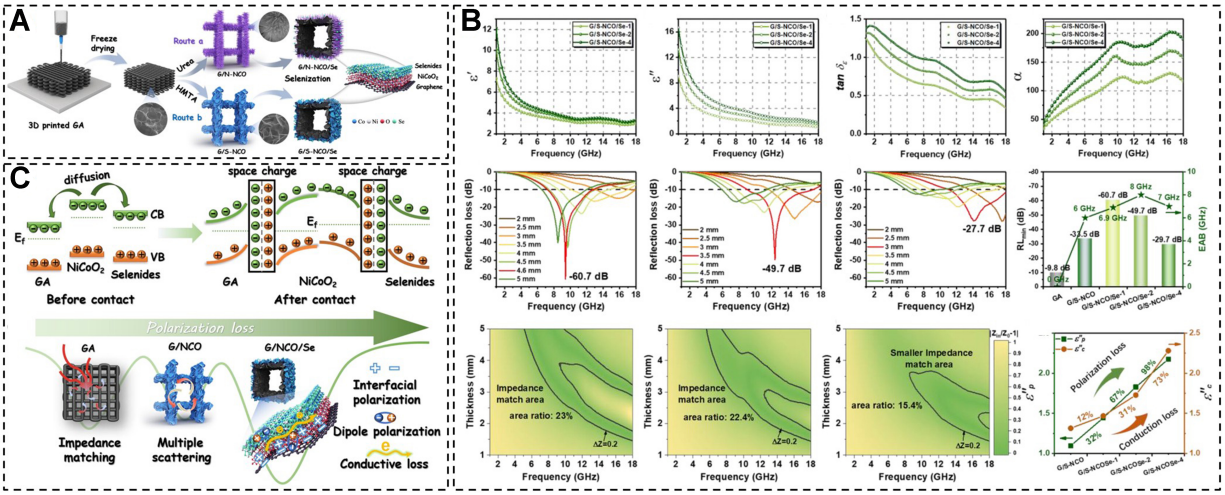

Figure 7. (A) Schematic diagram of the fabrication process, (B) microwave absorption performance, and (C) mechanism of 3D-printed graphene/$NiCoO_2$/Se materials[139]. Reproduced with permission[139]. Copyright 2024, American Chemical Society. 3D: Three-dimensional; GA: graphene aerogel; HMTA: hexamethylenetetramine; NCO: $NiCoO_2$; RL: reflection loss; EAB: effective absorption bandwidth.

Table 3. Comparison of microwave absorption performance of carbon-based aerogels with the non-template method

Sample	Mass ratio (%)	Optimal R_L value (dB)	*f* at optimal RL (GHz)	d (mm)	EAB (GHz)	Ref.
CSA-RGO AMs	4	-63.00	12.64	3.60	7.04	[135]
HCNTs@$Ti_3C_2T_x$	-	-35.50	10.60	2.20	2.20	[136]
MC-3	15	-53.02	9.28	3.80	4.44	[137]
CPDA@RCNFs	5	-63.31	~17.50	1.80	5.60	[138]
graphene/$NiCoO_2$/Se	-	-60.70	~9.00	4.60	8.00	[139]
MG2-1.4	-	-56.85	17.90	2.70	8.10	[140]

RL: Reflection loss; EAB: effective absorption bandwidth.

thermal insulation due to air trapped in the numerous pores, highlighting its broad application potential. Zhang *et al.* constructed multidimensional hierarchical networks through a series of processes including electrospinning, deacetylation, self-polymerization, and carbonization, achieving an ultra-high RL of -63.31 dB and a wide EAB of 5.60 GHz at a thickness of 1.8 mm[138].

With recent technological advancements, 3D printing has attracted increasing attention for its unique ability to create customized configurations that are difficult to achieve with traditional manufacturing techniques. Liu *et al.* adopted a 3D printing strategy to construct a graphene-based conductive scaffold [Figure 7], followed by *in situ* anchoring of $NiCoO_2$ and Se nanosheets onto the skeleton[139]. This effectively enhanced interfacial polarization and magnetic loss, resulting in a remarkable RL of -60.7 dB and a wide EAB of 8 GHz. Liu *et al.* constructed a flexible MXene/RGO aerogel through a new 3D printing technology, which possessed lightweight properties and could be placed on the head of a dandelion seed[140]. By adjusting the composition content and the microstructure parameters, the microwave absorption performance could be effectively enhanced, achieving an ultra-wide EAB of 8.10 GHz, covering most of the X-band and the entire Ku band, and the minimum RL value was -56.85 dB. As shown in Table 3, these new techniques offer a new insight into synthesizing carbon-based materials with controllable 3D porous structures and remarkable performance, presenting great potential in the next-generation microwave-absorbing candidates.

Table 4. Comparison of different synthesis methods of carbon-based aerogels across different parameters

Method	Cost	Process complexity	Current industrialization	Structural controllability	Scalability
Hard-template	2-3	2	5	2	4
Soft-template	3-4	3-4	3	3-4	3
Non-template	5	5	1	5	5 (future)

Comparison of different templated methods

Constructing carbon-based aerogels with tailored porosity, size distribution, and orientation can effectively regulate EM response behaviors by optimizing impedance matching, dielectric loss, and multiple internal reflections. Both structural simulations and experimental analyses can reveal structure-property relationships and guide the rational design of carbon-based aerogels with enhanced microwave absorption performance. Different templating strategies present advantages in terms of process complexity, structural controllability, cost, scalability, and practical application potential, as discussed below:

The synthesis of carbon-based aerogels via the hard-template strategy primarily involves template pretreatment, assembly of the carbon precursor on the template, and optional carbonization or template-removal steps. The hard-template approach offers advantages including facile procedures, ease of scalability for batch production, low cost, and wide template availability, demonstrating feasibility for industrial-scale applications. However, due to the inherent structural differences in natural templates, the resulting aerogels often suffer from poor customizability and limited control over pore structure and corresponding microwave absorption performance.

By comparison, as a representative soft-template approach, the freeze-drying strategy typically involves preparing a carbon-based solution, constructing ice crystals with specific structures, removing the template by sublimation, and performing potential post-treatment steps. This method enables effective design and regulation of the 3D conductive network and ordered pore structures, facilitating precise tuning of the EM parameters of carbon-based aerogels. However, industrial adoption is constrained by the high cost of freeze-drying equipment, substantial energy consumption during sublimation, and relatively low production efficiency. Moreover, the growth behavior of ice crystals during freezing is difficult to precisely control at the nanoscale through process parameter adjustment, leading to challenges in perfectly replicating the pore structure. Future efforts should focus on improving structural controllability and template-removal efficiency to enhance both manufacturing cost-effectiveness and property consistency of the aerogel-based products.

Emerging non-template strategies, such as electrospinning and 3D printing, can precisely construct complex 3D structures (including gradient or periodic lattice structures) with the assistance of intelligent digital modeling and automated equipment. These methods can effectively control EM response behaviors, optimizing impedance matching and synergistic dissipation for customized microwave absorption performance. The core challenge lies in regulating the coupling properties of the raw materials, including the viscosity, electrical conductivity, and surface tension of spinning solutions, or the rheological behavior of printing inks, which are crucial in determining both the structure and properties of the resulting carbon-based materials. Although relatively high cost and operational complexity currently limit widespread application, these methods represent the direction for advanced intelligent manufacturing, showing great promise for next-generation high-value applications, including 5G communications, flexible electronics, and wearable devices. The comparison of different synthesis strategies is summarized in Table 4, in which larger numbers indicate higher superiority of the parameters.

Multi-functional integration of carbon-based aerogel

By utilizing the synergistic effects of heterogeneous components and porous network structures, carbon-based microwave-absorbing aerogels demonstrate remarkable potential for integrating multiple functionalities.

Specifically, due to the low thermal conductivity of air, aerogels with nano- and micro-scale pores can effectively restrict heat conduction of gas molecules by forming a thermal insulation structure[141]. Furthermore, oriented pore channels can not only suppress thermal convection but also promote the propagation and dissipation of microwaves along the interconnected conductive networks, thereby enabling both microwave absorption and thermal insulation simultaneously[142]. For example, the anisotropic porous structure of carbon-based aerogels with axial through-holes can be constructed via bidirectional freezing and subsequent carbonization[143]. The interconnected conductive network with long-range ordered lamellar layers and interlamellar bridges effectively promotes conduction loss along the parallel axis while impeding heat flow in the vertical direction, achieving a high RL of -63.0 dB and broad EAB of 7.0 GHz with thermal insulation properties. Additionally, incorporating non-conductive thermal insulating components such as aramid nanofibers[144] or polyimide[145] to form an interpenetrating network with the conductive skeleton enhances thermal management, thereby integrating infrared stealth performance into the microwave-absorbing aerogel. Moreover, introducing MXene[146] components with both high electrical conductivity and low infrared emissivity, combined with a multi-layered structure with gradient EM response properties, results in an aerogel exhibiting an excellent RL of -60.1 dB at an ultrawide EAB of 14.1 GHz, along with compressibility. COMSOL Multiphysics® simulations were used to analyze the evolution of power loss density in each layer, verifying the contribution of the gradient structures to the overall performance.

Moreover, surface modifications can be regarded as effective strategies for multi-functionalization[147]. By biomimicking the micro/nano roughness of lotus leaves, the hydrophobicity of carbon-based aerogels can be enhanced through decoration with heterogeneous nanoparticles (Fe_3O_4/Fe/C[148], rare-earth oxide Nd_2O_3[149]), which prevents water molecules from infiltrating the porous structure and affecting dielectric loss, thereby endowing the aerogel with self-cleaning capabilities and stable microwave absorption performance under humid conditions. Additionally, SiO_2 and Al_2O_3 can be used as corrosion-resistant coatings[150]. For example, Hou *et al.* prepared magnetic graphene-based aerogels through self-assembly, chemical reduction, and freeze-drying, achieving a minimum RL of -51.3 dB and broad EAB of 6.64 GHz[151]. During chemical reduction, the hydrophilic functional groups on the RGO surface were significantly reduced, resulting in remarkable chemical inertness due to limited reactive groups, with enhanced corrosion resistance (low corrosion potential of -0.45 V under a corrosion current density of 3.3 μA). This allowed the aerogel to maintain stable microwave absorption performance after long-term immersion in NaCl solution, demonstrating potential for critical marine applications. Zhang *et al.* doped highly electronegative fluorine atoms onto graphene, synthesizing MXene/fluorinated graphene/cellulose nanofiber aerogels, which significantly extended dipole relaxation times, achieving an ultrawide EAB of 9.08 GHz at a relatively low thickness of 2.54 mm[152]. The hybrid aerogel exhibited multifunctionality: the parallel layered structure decorated with MXene nanosheets enhanced the Joule heating effect and compressive strength, while the aligned porous structure enabled infrared thermal camouflage.

Based on their high specific surface area and 3D interconnected pore structures, the multi-functionalization of carbon-based aerogels can be achieved either by incorporating functional nanofillers or by tailoring hetero-interfacial properties of the nanocomposites. This approach integrates microwave absorption with thermal management, mechanical reinforcement, flame retardancy, and environmental stability, enabling long-term practical applications under extreme conditions.

CONCLUSION AND OUTLOOK

In summary, based on the comprehensive analysis and discussion, carbon-based microwave-absorbing aerogels exhibit exceptional properties, including strong RL intensity, wide EAB, lightweight, and multifunctionality. This outstanding performance is attributed to the rational design of dielectric-magnetic coupling networks and hierarchical porous architectures, which enable superior impedance matching and integration of multiple microwave dissipation mechanisms. As a result, carbon-based aerogels can meet diverse application requirements, ranging from civilian electronics to military stealth technologies. Despite significant progress, several challenges remain to be addressed in future research:

I) Imitating and constructing biomimetic structures

Adopting biomimetic approaches can help reveal the relationships between structural configurations and the EM response of aerogel materials. Future research can draw inspiration from nature, including the hierarchical pore structure of diatomite, the robust and interconnected network of spider webs, or the photonic crystal structures of butterfly wings. By replicating such architectures and mimicking EM response behaviors, bio-inspired aerogels could control the transmission paths of EM waves with different refraction and scattering properties, while enabling effective conversion of EM energy via resonant absorption and interference. This strategy holds promise for enhancing the overall microwave absorption performance of carbon-based aerogels.

II) Performance controlling by artificial intelligence

The use of artificial intelligence (AI) tools can significantly improve the efficiency of MAM design. Microwave absorption performance is strongly influenced by multiple parameters, including composition, synthesis process, and microstructural features. Traditional trial-and-error methods are often inefficient and imprecise, whereas AI-assisted machine learning models can construct comprehensive parameter databases and uncover structure-property relationships. Microwave response behaviors can be accurately predicted based on given aerogel parameters, supporting the inverse design of aerogel systems with targeted RL intensity and absorption frequency bands.

III) Multifunctional integration and intelligent response

Integrating diverse functionalities into carbon-based microwave-absorbing aerogels - including thermal management, hydrophobicity, corrosion resistance, and self-monitoring - is essential for practical applications under extreme conditions, ensuring long-term stability and reliability. Moreover, developing intelligent aerogels with active-responsive properties could allow reversible adjustment of EM parameters in response to external EM fields, dynamically tuning the effective absorption frequency range. This adaptive stealth functionality is critical for next-generation intelligent aerogel materials in advanced equipment.

IV) Large-scale production technology

The hard-template strategy offers advantages in cost-effectiveness and processing efficiency, making it compatible with scale-up and batch production, and has achieved success in industrial applications. In contrast, industrial adoption of soft-template strategies, such as freeze-drying, is limited by high equipment costs, energy consumption, and low production efficiency. Template-free strategies, including 3D printing and electrospinning, enable unprecedented spatial precision in controlling pore structures and geometry, holding significant potential for scalable manufacturing. Therefore, developing eco-friendly, low-cost, and scalable synthesis routes is essential to promote practical applications of carbon-based aerogels in both military and civilian fields.

DECLARATIONS

Authors' contributions

Conceptualization and manuscript design: Wang, K.

Literature search and data collection: Wang, K.; Liu, X.

Writing - original draft preparation: Wang, K.; Chu, W.
Visualization and figure preparation: Li, X.
Review and editing: Liu, H.; Wang, K.

Availability of data and materials

Not applicable.

Financial support and sponsorship

Wang, K. acknowledges support from the National Natural Science Foundation of China (No. 52302364) and the China Postdoctoral Science Foundation (No. 2023T160413).

Conflicts of interest

All authors declared that there are no conflicts of interest.

Ethical approval and consent to participate

Not applicable.

Consent for publication

Not applicable.

REFERENCES

1. Cao, W.; Wang, X.; Yuan, J.; Wang, W.; Cao, M. Temperature dependent microwave absorption of ultrathin graphene composites. *J. Mater. Chem. C.* **2015**, *3*, 10017-22. DOI
2. Wang, X.; Ma, T.; Shu, J.; Cao, M. Confinedly tailoring Fe_3O_4 clusters-NG to tune electromagnetic parameters and microwave absorption with broadened bandwidth. *Chem. Eng. J.* **2018**, *332*, 321-30. DOI
3. Du, Y.; Liu, Y.; Wang, A.; Kong, J. Research progress and future perspectives on electromagnetic wave absorption of fibrous materials. *iScience* **2023**, *26*, 107873. DOI PubMed PMC
4. Ran, S.; Sun, K.; Zhao, M.; et al. Metal-organic framework derived carbon-based composites for high-performance microwave absorption. *Adv. Compos. Hybrid. Mater.* **2025**, *8*, 1077. DOI
5. Hao, B.; Chai, Z.; Li, M.; et al. Design of mesoscopic metacomposites for electromagnetic wave absorption: enhancing performance and gaining mechanistic insights. *Soft. Sci.* **2025**, *5*, 39. DOI
6. Wang, C.; Murugadoss, V.; Kong, J.; et al. Overview of carbon nanostructures and nanocomposites for electromagnetic wave shielding. *Carbon* **2018**, *140*, 696-733. DOI
7. Zhang, Y.; Wang, X.; Cao, M. Confinedly implanted $NiFe_2O_4$-rGO: cluster tailoring and highly tunable electromagnetic properties for selective-frequency microwave absorption. *Nano. Res.* **2018**, *11*, 1426-36. DOI
8. Zeng, X.; Zhao, C.; Yin, Y.; et al. Construction of $NiCo_2O_4$ nanosheets-covered $Ti_3C_2T_x$ MXene heterostructure for remarkable electromagnetic microwave absorption. *Carbon* **2022**, *193*, 26-34. DOI
9. Wen, L.; Guan, L.; Zhang, J.; et al. Defect engineering boosts microwave absorption in $Ta_xNb_{1-x}C$ nanowires. *Rare. Met.* **2025**, *44*, 2577-88. DOI
10. Ren, S.; Pan, S.; Jin, Y.; et al. Magnetoelectric characterisation of $SrFe_{12}O_{19}$@MoS_2 composites with high microwave absorption performance. *Ceram. Int.* **2025**, *51*, 10184-92. DOI
11. Kim, S.; Kim, S.; Yoon, Y.; Lee, K. Magnetic, dielectric, and microwave absorbing properties of iron particles dispersed in rubber matrix in gigahertz frequencies. *J. Appl. Phys.* **2005**, *97*, 10F905. DOI
12. Gao, B.; Qiao, L.; Wang, J.; et al. Microwave absorption properties of the Ni nanowires composite. *J. Phys. D. Appl. Phys.* **2008**, *41*, 235005. DOI
13. Liu, Y.; Geng, W.; Wang, L.; et al. Designing MXene hydrogels for flexible and high-efficiency electromagnetic wave absorption using digital light processing 3D printing. *Chem. Eng. J.* **2025**, *505*, 159489. DOI
14. He, Y.; Su, Q.; Liu, D.; et al. Surface engineering strategy for MXene to tailor electromagnetic wave absorption performance. *Chem. Eng. J.* **2024**, *491*, 152041. DOI

15. Zhan, B.; Qi, X.; Yang, J.; et al. Advancing microwave absorption: innovative strategies spanning nano-micro engineering to metamaterial design. *Nano. Res.* **2025**, *18*, 94907209. DOI
16. Zhao, J.; Gu, Z.; Zhang, Q. Stacking MoS_2 flower-like microspheres on pomelo peels-derived porous carbon nanosheets for high-efficient X-band electromagnetic wave absorption. *Nano. Res.* **2024**, *17*, 1607-15. DOI
17. Wu, N.; Shen, Z.; Ma, Y.; et al. Three-dimensional lightweight melamine foams modified by MXene sheets and CoNi alloys towards multifunctional microwave absorption. *Nano. Res.* **2025**, *18*, 94907121. DOI
18. Zhang, J.; Xia, L.; Yang, L.; et al. $Ti_3C_2T_x$ MXene nanobelts with alkali ion intercalation: dual-purpose for enhanced lithium-ion batteries and microwave absorption. *Carbon* **2025**, *237*, 120148. DOI
19. Wang, D.; Ping, T.; Du, Z.; Liu, X.; Zhang, Y. Lessons from nature: advances and perspectives in bionic microwave absorption materials. *Nanomicro. Lett.* **2024**, *17*, 100. DOI PubMed PMC
20. Ma, Z.; Yang, K.; Li, D.; et al. The electron migration polarization boosting electromagnetic wave absorption based on Ce atoms modulated yolk@shell Fe_xN@NGC. *Adv. Mater.* **2024**, *36*, e2314233. DOI PubMed
21. Zhang, Z.; Kong, Y.; Zhang, J.; Hou, J.; Cao, M.; Wang, X. Recent progress of microwave absorption motivated by metal single atoms anchored on two-dimensional materials. *Carbon* **2025**, *235*, 120095. DOI
22. Hao, B.; Zhang, Y.; Si, H.; et al. Multiscale design of dielectric composites for enhanced microwave absorption performance at elevated temperatures. *Adv. Funct. Mater.* **2025**, *35*, 2423897. DOI
23. Sun, X.; Wu, Z.; Tan, X.; et al. In situ "work-invaliding-awakened" of reduced graphene oxide/SiO_2 bilayer aerogels for broadband microwave absorption based on thermally reduced reconstructed carbon networks. *Adv. Funct. Mater.* **2025**, *35*, e12145. DOI
24. Li, Q.; Liu, L.; Kimura, H.; et al. Interfacical polarization dominant rGO aerogel decorated with molybdenum sulfide towards lightweight and high-performance electromagnetic wave absorber. *Carbon* **2025**, *231*, 119738. DOI
25. Shu, R.; Xu, L.; Guan, Y. Preparation of cellulose derived carbon/reduced graphene oxide composite aerogels for broadband and efficient microwave dissipation. *J. Colloid. Interface. Sci.* **2024**, *675*, 401-10. DOI PubMed
26. Li, J.; Xu, Z.; Li, T.; et al. Multifunctional antimony tin oxide/reduced graphene oxide aerogels with wideband microwave absorption and low infrared emissivity. *Compos. Part. B. Eng.* **2022**, *231*, 109565. DOI
27. He, M.; Zhang, K.; Qiu, H.; et al. Low-frequency microwave absorption composites. *Adv. Sci.* **2025**, *12*, e11580. DOI PubMed PMC
28. Chen, X.; Wang, W.; Su, R.; Huang, Y.; Li, Y.; He, R. 3D-printed electromagnetic microwave absorption structures: a comprehensive review. *J. Mater. Chem. A.* **2025**, *13*, 22240-70. DOI
29. Zeng, X.; Cheng, X.; Yu, R.; Stucky, G. D. Electromagnetic microwave absorption theory and recent achievements in microwave absorbers. *Carbon* **2020**, *168*, 606-23. DOI
30. Liu, J.; Pan, Y.; Yu, L.; et al. MoS_2-based composites for microwave absorption mechanism-oriented structural optimization and design perspectives. *Carbon* **2025**, *238*, 120233. DOI
31. Ma, Y.; Wei, S.; Liu, R.; Sun, L.; Wang, W. A review on MXene-based microwave absorption composites: engineering, component optimization and structure regulation. *J. Mater. Chem. C.* **2024**, *12*, 9068-93. DOI
32. Jiang, W.; Jiang, D.; Huang, Y.; Jiang, B. Strategies to construct conductive structures of polymer-based electromagnetic wave attenuation composites. *J. Mater. Chem. A.* **2024**, *12*, 4383-96. DOI
33. Han, M.; Lan, D.; Zhang, Z.; et al. Micro-sized hexapod-like CuS/Cu_9S_5 hybrid with broadband electromagnetic wave absorption. *J. Mater. Sci. Technol.* **2025**, *214*, 302-12. DOI
34. Jian, S.; Wu, X.; Yu, H.; Wang, L. Enhancing strategies of MOFs-derived materials for microwave absorption: review and perspective. *Adv. Colloid. Interface. Sci.* **2025**, *338*, 103412. DOI
35. Chu, W.; Wang, K.; Liu, S.; Chen, Y.; Li, H.; Liu, H. Tailorable effective microwave absorption bandwidth of chitosan-derived carbon-based aerogel under different compression. *Mater. Res. Bull.* **2024**, *177*, 112857. DOI
36. Wang, K.; Chu, W.; Li, H.; Chen, Y.; Cai, Y.; Liu, H. Ferromagnetic Ti_3CNCl_2-decorated RGO aerogel: from 3D interconnecting conductive network construction to ultra-broadband microwave absorber with thermal insulation property. *J. Colloid. Interface. Sci.* **2021**, *604*, 402-14. DOI PubMed
37. Wu, Z.; Huang, J.; Zeng, X. Dual magnetic particles modified carbon nanosheets in CoFe/Co@NC heterostructure for efficient electromagnetic synergy. *Soft. Sci.* **2024**, *4*, 42. DOI
38. Chu, W.; Wang, K.; Li, H.; Chen, Y.; Liu, H. Harvesting yolk-shell nanocomposites from Fe-MIL-101 self-template in NaCl/KCl molten salt environment for high-performance microwave absorber. *Chem. Eng. J.* **2022**, *430*, 133112. DOI
39. Wang, K.; Chu, W.; Chen, Y.; Li, H.; Liu, H. Maintaining electromagnetic interference shielding and flame-retardant performance of recycled carbon fiber-reinforced composites under multiple pyrolysis recycles. *Compos. Sci. Technol.* **2024**, *248*, 110470. DOI
40. Wang, K.; Chen, C.; Zheng, Q.; et al. Multifunctional recycled carbon fiber-$Ti_3C_2T_x$ MXene paper with superior electromagnetic interference shielding and photo/electro-thermal conversion performances. *Carbon* **2022**, *197*, 87-97. DOI

41. Shen, Z.; Lan, D.; Cong, Y.; Lian, Y.; Wu, N.; Jia, Z. Tailored heterogeneous interface based on porous hollow In-Co-C nanorods to construct adjustable multi-band microwave absorber. *J. Mater. Sci. Technol.* **2024**, *181*, 128-37. DOI
42. Ren, X.; Zhen, M.; Meng, F.; Meng, X.; Zhu, M. Progress, challenges and prospects of biomass-derived lightweight carbon-based microwave-absorbing materials. *Nanomaterials* **2025**, *15*, 553. DOI PubMed PMC
43. Hao, Z.; Zhou, J.; Lin, S.; et al. Customized heterostructure of transition metal carbides as high-efficiency and anti-corrosion electromagnetic absorbers. *Carbon* **2024**, *228*, 119323. DOI
44. Wu, Z.; Huang, J.; Tan, Y.; Deng, X.; Zeng, X. Transition/rare earth metal co-modified SiC for low-frequency and high-temperature electromagnetic response. *J. Adv. Ceram.* **2025**, *14*, 9221164. DOI
45. Liu, A.; Xu, X.; Qiu, H.; et al. Bioinspired hollow heterostructure fillers for enhanced electromagnetic interference shielding in polyimide aerogels. *InfoMat* **2025**, *7*, e70060. DOI
46. Naqvi, S. T. A.; Singh, C.; Godara, S. K. Functionalization and synthesis of biomass and its composites as renewable, lightweight and eco-efficient microwave-absorbing materials: a review. *J. Alloys. Compd.* **2023**, *968*, 171991. DOI
47. Mei, J.; Luo, J.; Zhao, T.; et al. Morphology engineering of MIL-88A-derived 0D/1D/2D nanocomposites toward wideband microwave absorption. *J. Mater. Sci. Technol.* **2025**, *226*, 65-75. DOI
48. Cao, R.; Qiu, Y.; Zhao, X.; et al. Carbon-$CoFe_2O_4$ composite with hierarchical porous structure for efficient microwave absorption. *Diam. Relat. Mater.* **2025**, *157*, 112542. DOI
49. Wang, L.; Huang, M.; Rao, L.; et al. Atomically polarization regulation in molybdenum disulfide nanosheets via phase transition engineering for superior electromagnetic wave dissipation. *Adv. Funct. Mater.* **2025**, *35*, 2507569. DOI
50. Zhang, Y.; Yu, H.; Wang, L.; et al. Research progress on conductive polymer-based microwave absorption materials: from materials design to functionalities and applications. *Mater. Horiz.* **2025**, *12*, 10029-58. DOI PubMed
51. Chen, J.; Zhang, J.; Wang, X.; et al. Alkalized chemical scissors form honeycomb MXene for enhanced microwave absorption performance. *J. Alloys. Compd.* **2025**, *1036*, 181872. DOI
52. Huang, J.; Xu, Z.; Chen, Z.; Liu, Z.; Yuan, G. Preparation of FeSiMn composites and study on the microwave absorption performance. *J. Alloys. Compd.* **2025**, *1021*, 179641. DOI
53. Shu, R.; Guan, Y.; Liu, B. Preparation of nitrogen-doped reduced graphene oxide/zinc ferrite@nitrogen-doped carbon composite for broadband and highly efficient electromagnetic wave absorption. *J. Mater. Sci. Technol.* **2025**, *214*, 16-26. DOI
54. Li, J.; Lan, D.; Cheng, Y.; et al. Constructing mixed-dimensional lightweight magnetic cobalt-based composites heterostructures: an effective strategy to achieve boosted microwave absorption and self-anticorrosion. *J. Mater. Sci. Technol.* **2024**, *196*, 60-70. DOI
55. Wang, G.; Gao, Z.; Wan, G.; Lin, S.; Yang, P.; Qin, Y. High densities of magnetic nanoparticles supported on graphene fabricated by atomic layer deposition and their use as efficient synergistic microwave absorbers. *Nano. Res.* **2014**, *7*, 704-16. DOI
56. Zhao, B.; Lan, D.; Zhang, M.; Liu, L.; Wu, N.; Yao, S. Multiphase interface engineering based on porous manganous oxide toward broad-band microwave absorption. *Mater. Res. Bull.* **2024**, *171*, 112621. DOI
57. Zhang, S.; Zheng, J.; Lv, C.; et al. Synergistic enhancement of defect-induced polarization and built-in electric field effect in carbon hybrids towards efficient electromagnetic wave absorption. *Carbon* **2025**, *234*, 120037. DOI
58. Xie, L.; Liu, R.; Jiang, X.; et al. Carbon induced multiple interfaces and in-situ formed defects in oxidation of Co toward enhancing microwave absorption performances. *Carbon* **2025**, *238*, 120272. DOI
59. Ren, J.; Shi, P.; Zu, X.; et al. Challenges and future prospects of the 2D material-based composites for microwave absorption. *Nanoscale* **2025**, *17*, 13622-45. DOI PubMed
60. Guo, Z.; Zhang, X.; Lv, C.; et al. Advantageous synergistic strategy to construct Ni@C/PC composites for efficient electromagnetic wave absorption. *Carbon* **2025**, *234*, 120010. DOI
61. Tariq, M. R.; Ahmad, M.; Naik, M.; Khan, I.; Zhang, B. A comprehensive review of the advancement of transition metal oxide nanocomposites for microwave absorption. *Coord. Chem. Rev.* **2025**, *533*, 216535. DOI
62. Zhou, Z.; Lan, D.; Ren, J.; et al. Controllable heterogeneous interfaces and dielectric modulation of biomass-derived nanosheet metal-sulfide complexes for high-performance electromagnetic wave absorption. *J. Mater. Sci. Technol.* **2024**, *185*, 165-73. DOI
63. Jiang, B.; Shang, J.; Zhang, F.; et al. Electrospinning fabrication of hollow C@TiO_2/Fe_3C nanofibers composites for excellent wave absorption at a low filling content. *Chem. Eng. J.* **2024**, *495*, 153663. DOI
64. Hu, J.; Jiang, J.; Li, Q.; et al. Metal–organic framework-based composites for dual functionalities: advances in microwave absorption and flame retardancy. *J. Compos. Sci.* **2025**, *9*, 121. DOI
65. Wu, D.; Fan, C.; Luo, W.; Jin, Y.; He, Q.; Wang, Y. Enhanced interfacial polarization loss induced by hollow engineering of hollow alloyed CoFe-ZIF nanocages/carbon nanofibers for efficient microwave absorption. *Inorg. Chem. Front.* **2025**, *12*, 3083-97. DOI
66. Zhang, D.; He, W.; Quan, G.; et al. Sterculia lychnophora seed-derived porous carbon@$CoFe_2O_4$ composites with efficient microwave absorption performance. *Appl. Surf. Sci.* **2023**, *607*, 155027. DOI

67. Xia, Y.; Gao, W.; Gao, C. A review on graphene-based electromagnetic functional materials: electromagnetic wave shielding and absorption. *Adv. Funct. Mater.* **2022**, *32*, 2204591. DOI
68. Ding, H.; Hu, B.; Wang, Y.; Du, Y. Current progress and frontiers in three-dimensional macroporous carbon-based aerogels for electromagnetic wave absorption: a review. *Nanoscale* **2024**, *16*, 21731-60. DOI PubMed
69. Wang, H.; Xiao, J.; Qi, X.; et al. Microstructural optimization and non-metallic doping strategy to develop mesoporous N-doped carbon hollow nanospheres for strong and broadband microwave absorption. *J. Mater. Sci. Technol.* **2026**, *247*, 55-63. DOI
70. Qiao, J.; Song, Q.; Zhang, X.; et al. Enhancing interface connectivity for multifunctional magnetic carbon aerogels: an in situ growth strategy of metal-organic frameworks on cellulose nanofibrils. *Adv. Sci.* **2024**, *11*, e2400403. DOI PubMed PMC
71. Zeng, X.; Peng, X.; Ning, Y.; Jiang, X.; Yu, R.; Zhang, X. 3D multifunctional porous pine carbon aerogels coupled with highly dispersed CoFe nanoparticles for robust electromagnetic wave response. *J. Mater. Sci. Technol.* **2024**, *192*, 6-18. DOI
72. Ai, Y.; Xing, R.; Ren, N.; et al. Biomass-derived hierarchical carbon frameworks enable robust microwave absorption. *Matter* **2025**, *8*, 102289. DOI
73. Zhao, L.; Zhuang, Q.; Hu, G.; Zhang, B.; Pan, S. Ni/porous carbon-based composite derived from poplar wood with ultrabroad band microwave absorption performance. *ECS. J. Solid. State. Sci. Technol.* **2024**, *13*, 021004. DOI
74. Gou, G.; Hua, W.; Liu, K.; Cheng, F.; Xie, X. Bimetallic MOF@wood-derived hierarchical porous carbon composites for efficient microwave absorption. *Diam. Relat. Mater.* **2024**, *141*, 110688. DOI
75. Cui, A.; Miao, Y.; Wang, C.; et al. $NiFe_2O_4$/Ni_3Fe nanoparticles Decorate wood carbon strategies for efficient electromagnetic absorption. *Chem. Eng. J.* **2025**, *507*, 160354. DOI
76. Cui, C.; Geng, L.; Jiang, S.; et al. Architecture design of a bamboo cellulose/Nb_2CT_x MXene/ZIF-67-derived lightweight Co/Nb_2CT_x/carbon aerogel for highly efficient electromagnetic wave absorption, thermal insulation, and flame retardant. *Ind. Eng. Chem. Res.* **2023**, *62*, 8297-311. DOI
77. Shen, M.; Li, X.; Qi, J.; et al. Magnetic metal-loaded wood carbon aerogel composites for electromagnetic shielding and microwave absorption. *Compos. Part. A. Appl. Sci. Manuf.* **2025**, *198*, 109070. DOI
78. Xiao, J.; Wen, B.; Liu, X.; et al. In-situ growth of carbon nanotubes for the modification of wood-derived biomass porous carbon to achieve efficient Low/Mid-Frequency electromagnetic wave absorption. *J. Colloid. Interface. Sci.* **2024**, *676*, 33-44. DOI PubMed
79. Cheng, Y.; Zhao, H.; Lv, H.; Shi, T.; Ji, G.; Hou, Y. Lightweight and flexible cotton aerogel composites for electromagnetic absorption and shielding applications. *Adv. Elect. Mater.* **2020**, *6*, 1900796. DOI
80. Huang, X.; Wang, Y.; Lou, Z.; Chen, Y.; Li, Y.; Lv, H. Porous, magnetic carbon derived from bamboo for microwave absorption. *Carbon* **2023**, *209*, 118005. DOI
81. Chang, Q.; Xie, Z.; Long, C.; Feng, X.; Shi, B.; Wu, H. Magnetic hierarchically porous biomass carbon for realizing broadband and strong absorption of electromagnetic wave. *Ceram. Int.* **2023**, *49*, 27015-23. DOI
82. Li, Z.; Liang, J.; Wei, Z.; et al. Lightweight foam-like nitrogen-doped carbon nanotube complex achieving highly efficient electromagnetic wave absorption. *J. Mater. Sci. Technol.* **2024**, *168*, 114-23. DOI
83. Yu, J.; Luo, H.; Wang, Z.; et al. Surface morphology of magnetic carbon foam regulated electromagnetic properties for microwave absorption. *J. Alloys. Compd.* **2024**, *971*, 172757. DOI
84. Yu, J.; Luo, H.; Lv, S.; et al. Facile fabrication of melamine/MXene/FeNi-PBA composite derived multi-interface magnetic carbon foam for high-efficiency microwave absorption. *Adv. Elect. Mater.* **2025**, *11*, 2400265. DOI
85. Jia, T.; Qi, X.; Wang, L.; et al. Constructing mixed-dimensional lightweight flexible carbon foam/carbon nanotubes-based heterostructures: an effective strategy to achieve tunable and boosted microwave absorption. *Carbon* **2023**, *206*, 364-74. DOI
86. Rong, H.; Song, H.; Gao, T.; Li, Y.; Zhao, R.; Zhang, X. Ultralight melamine foam derived metal nanoparticles encapsulated CNTs/porous carbon composite for electromagnetic absorption. *Synth. Met.* **2023**, *294*, 117306. DOI
87. Zhu, X.; Dong, Y.; Xiang, Z.; et al. Morphology-controllable synthesis of polyurethane-derived highly cross-linked 3D networks for multifunctional and efficient electromagnetic wave absorption. *Carbon* **2021**, *182*, 254-64. DOI
88. Lou, Z.; Li, R.; Wang, P.; et al. Phenolic foam-derived magnetic carbon foams (MCFs) with tunable electromagnetic wave absorption behavior. *Chem. Eng. J.* **2020**, *391*, 123571. DOI
89. Shao, G.; Yang, Y.; Jia, S.; et al. Covalent organic framework-amplified polarization loss in ultralight Schottky heterojunction aerogels for low-frequency electromagnetic wave absorption. *Adv. Funct. Mater.* **2025**, e16078. DOI
90. Guo, Y.; Wang, D.; Tian, Y.; et al. FeCo alloy nanoparticle decorated cellulose based carbon aerogel as a low-cost and efficient electromagnetic microwave absorber. *J. Mater. Chem. C.* **2021**, *10*, 126-34. DOI
91. Yang, P.; Wang, L.; Ruan, H.; et al. Heterogeneous interface engineering and directional tuning electromagnetic parameters of MXene/Fe NPs absorbers for precise low-frequency microwave absorption. *Nano. Res.* **2025**, *18*, 94907783. DOI

92. Zhu, C.; An, X.; Wang, J.; Chen, Y.; Nan, K.; Wang, Y. Dimensional design of cellulose aerogels with Schottky contact for efficient microwave absorption. *Small* **2025**, *21*, e2411743. DOI PubMed
93. Wang, B.; Nan, K.; Rao, H.; Chen, Y.; Pei, R.; Wang, Y. Integrated design of multifunctional lightweight magnetic cellulose-based aerogel with 1D/2D/3D hierarchical network for efficient microwave absorption. *Compos. Commun.* **2024**, *49*, 101987. DOI
94. Su, X.; Wang, J.; Liu, T.; et al. Controllable atomic migration in microstructures and defects for electromagnetic wave absorption enhancement. *Adv. Funct. Mater.* **2024**, *34*, 2403397. DOI
95. Liu, F.; Cai, Z.; Li, Z.; et al. Chitosan/MXene/Co_3O_4-derived composite aerogels with hierarchically porous structure for electromagnetic wave absorption. *Appl. Surf. Sci.* **2025**, *689*, 162550. DOI
96. Ren, X.; Huang, L.; Yuan, H.; et al. Sodium alginate derived SiC-carbon composite aerogel for effective microwave absorption. *J. Magn. Magn. Mater.* **2024**, *596*, 171970. DOI
97. Xiang, L.; Pan, D.; Lei, J.; et al. Sodium alginate aerogel derived SiC@Co-C 3D network enhances electromagnetic wave absorption and thermal conductivity of PDMS based composite. *Int. J. Biol. Macromol.* **2025**, *306*, 141539. DOI
98. Jiang, Y.; Cheng, H.; Liu, X.; Ai, Y.; He, A.; Nie, H. High-performance honeycomb porous microwave absorbers: gelatin-based carbon nanotube/nickel nanowire aerogels. *J. Alloys. Compd.* **2025**, *1010*, 177341. DOI
99. Zhou, X.; Wang, B.; Jia, Z.; et al. Dielectric behavior of Fe_3N@C composites with green synthesis and their remarkable electromagnetic wave absorption performance. *J. Colloid. Interface. Sci.* **2021**, *582*, 515-25. DOI
100. Liu, J.; Zhang, S.; Qu, D.; et al. Defects-rich heterostructures trigger strong polarization coupling in sulfides/carbon composites with robust electromagnetic wave absorption. *Nanomicro. Lett.* **2024**, *17*, 24. DOI PubMed PMC
101. Luo, Z.; Gu, W.; He, J.; Shen, L.; Ji, G. Construction of dielectric and magnetic coupling cobalt salt/chitosan derived Co/C hybrid aerogels for high-performance infrared/radar compatible applications. *Ceram. Int.* **2024**, *50*, 45427-37. DOI
102. Peng, L.; Yu, H.; Chen, C.; et al. Tailoring dense, orientation-tunable, and interleavedly structured carbon-based heat dissipation plates. *Adv. Sci.* **2023**, *10*, e2205962. DOI PubMed PMC
103. Guo, Y.; Duan, Y.; Liu, X.; et al. Construction of rGO/MOF-derived CNTs aerogel with multiple losses for multi-functional efficient electromagnetic wave absorber. *Carbon* **2024**, *230*, 119591. DOI
104. Cao, K.; Ye, W.; Fang, Y.; Zhang, Y.; Zhao, R.; Xue, W. Construction of three-dimensional porous network Fe-rGO aerogels with monocrystal magnetic Fe_3O_4@C core-shell structure nanospheres for enhanced microwave absorption. *Mater. Today. Phys.* **2024**, *42*, 101383. DOI
105. Nguyen, L. T.; Goh, C. J.; Bai, T.; Ong, R. H.; Goh, X. Y.; Duong, H. M. Scalable fabrication of lightweight carbon nanotube aerogel composites for full X-band electromagnetic wave absorption. *Carbon* **2024**, *219*, 118811. DOI
106. Wang, P.; Fan, D.; Gai, L.; et al. Synthesis of graphene oxide-mediated high-porosity Ni/C aerogels through topological MOF deformation for enhanced electromagnetic absorption and thermal management. *J. Mater. Chem. A.* **2024**, *12*, 8571-82. DOI
107. Shu, Y.; Zhao, T.; Li, X.; et al. Enhancing electromagnetic wave absorption and hydrophobicity/heat insulation properties of coral-like Co/CoO/RGO aerogels through pore structure regulation. *Carbon* **2023**, *213*, 118278. DOI
108. Shi, T.; Yao, Y.; Li, Y.; Lu, S.; Qin, W.; Wu, X. Inner phase hybridization engineering of core-shell structure confined in graphene scroll for boosting electromagnetic wave absorption. *Chem. Eng. J.* **2023**, *455*, 140683. DOI
109. Wang, H.; Liu, D.; Zhang, K.; et al. Shape memory HCNTs/PANI/WPU aerogels as dynamically tunable microwave absorbers in response to mechanical deformation. *J. Alloys. Compd.* **2025**, *1036*, 181930. DOI
110. Fei, Y.; Wang, X.; Yuan, M.; Liang, M.; Chen, Y.; Zou, H. Co nanoparticles encapsulated in carbon nanotubes decorated carbon aerogels toward excellent microwave absorption. *Ind. Eng. Chem. Res.* **2022**, *61*, 1684-93. DOI
111. Li, X.; Zhu, L.; Kasuga, T.; Nogi, M.; Koga, H. Chitin-derived-carbon nanofibrous aerogel with anisotropic porous channels and defective carbon structures for strong microwave absorption. *Chem. Eng. J.* **2022**, *450*, 137943. DOI
112. Li, X.; Zhu, L.; Kasuga, T.; Nogi, M.; Koga, H. Frequency-tunable and absorption/transmission-switchable microwave absorber based on a chitin-nanofiber-derived elastic carbon aerogel. *Chem. Eng. J.* **2023**, *469*, 144010. DOI
113. Zhi, D.; Li, T.; Qi, Z.; et al. Core-shell heterogeneous graphene-based aerogel microspheres for high-performance broadband microwave absorption via resonance loss and sequential attenuation. *Chem. Eng. J.* **2022**, *433*, 134496. DOI
114. Cui, Y.; Yang, K.; Wang, J.; Shah, T.; Zhang, Q.; Zhang, B. Preparation of pleated RGO/MXene/Fe_3O_4 microsphere and its absorption properties for electromagnetic wave. *Carbon* **2021**, *172*, 1-14. DOI
115. Yu, C.; Guo, J.; Lv, S.; Jiang, X. Modified zirconia fiber/reduced graphene oxide composite aerogels with exceptional mechanical and microwave absorption properties for harsh-environment applications. *Chem. Eng. J.* **2023**, *468*, 143850. DOI
116. Liang, L.; Li, Q.; Yan, X.; et al. Multifunctional Magnetic $Ti_3C_2T_x$ MXene/graphene aerogel with superior electromagnetic wave absorption performance. *ACS. Nano.* **2021**, *15*, 6622-32. DOI PubMed

117. Chen, Y.; Gai, L.; Hu, B.; et al. Directional three-dimensional macroporous carbon foams decorated with WC_{1-x} nanoparticles derived from salting-out protein assemblies for highly effective electromagnetic absorption. *Nanomicro. Lett.* **2025**, *18*, 71. DOI PubMed PMC
118. Wang, J.; Xia, M.; Sun, J.; et al. Hybrid bilayers of carbon/$NiBr_2$ anchoring on FeSiB surface for enhanced microwave absorption coupling with smart discoloration. *Rare. Met.* **2025**, *44*, 489-502. DOI
119. Lin, X.; Wang, C.; Zhang, C.; et al. Asymmetric gradient-structured PPy@bacterial nanocellulose aerogels enable broadband microwave absorption via synergistic polarization-conduction loss. *Chem. Eng. J.* **2025**, *520*, 166529. DOI
120. Zhang, J.; Zhang, Z.; Liu, L.; et al. Dual-gradient Mo_2C-decorated rGO aerogels for enhanced electromagnetic wave absorption. *J. Alloys. Compd.* **2025**, *1010*, 177683. DOI
121. Hang, T.; Zhou, L.; Li, Z.; et al. Constructing gradient reflection and scattering porous framework in composite aerogels for enhanced microwave absorption. *Carbohydr. Polym.* **2024**, *329*, 121777. DOI
122. Pan, H.; Yin, X.; Xue, J.; Cheng, L.; Zhang, L. In-situ synthesis of hierarchically porous and polycrystalline carbon nanowires with excellent microwave absorption performance. *Carbon* **2016**, *107*, 36-45. DOI
123. Xu, J.; Ma, Z.; Yang, P.; Zhu, C.; Chen, Y. 3D hierarchically ordered porous carbon frameworks/Co nanoparticles for Broadening electromagnetic wave absorption bandwidth. *Carbon* **2025**, *233*, 119916. DOI
124. Zhang, M.; Ling, H.; Wang, T.; et al. An equivalent substitute strategy for constructing 3D ordered porous carbon foams and their electromagnetic attenuation mechanism. *Nanomicro. Lett.* **2022**, *14*, 157. DOI PubMed PMC
125. Xiao, J.; Wen, B.; Li, J.; et al. Engineering of N doped carbon@FeCo alloy hollow spheres: remarkable mid-frequency electromagnetic wave absorption performance exhibited by unique porous and wrinkled surface structure. *J. Alloys. Compd.* **2024**, *1008*, 176595. DOI
126. Chen, J.; Wu, S.; Guanxu, Q.; et al. Modulation of pore size to enhance electromagnetic wave absorption in 3D ordered macroporous materials. *J. Mater. Sci. Mater. Electron.* **2025**, *36*, 14123. DOI
127. Xu, R.; Xu, D.; Zeng, Z.; Liu, D. $CoFe_2O_4$/porous carbon nanosheet composites for broadband microwave absorption. *Chem. Eng. J.* **2022**, *427*, 130796. DOI
128. Li, F.; Bi, Z.; Kimura, H.; et al. Energy- and cost-efficient salt-assisted synthesis of nitrogen-doped porous carbon matrix decorated with nickel nanoparticles for superior electromagnetic wave absorption. *Adv. Compos. Hybrid. Mater.* **2023**, *6*, 710. DOI
129. Wei, Q.; Huang, Y.; Dong, L.; et al. Fe_3O_4 nanoparticles embedded into pyridinic-N-rich carbon nanohoneycomb with strong dx^2-Pz orbital hybridization for high-performance electromagnetic wave absorption. *ACS. Appl. Mater. Interfaces.* **2024**, *16*, 38414-28. DOI PubMed
130. Guo, R.; Zheng, Q.; Wang, L.; Fan, Y.; Jiang, W. Porous N-doped Ni@SiO_2/graphene network: three-dimensional hierarchical architecture for strong and broad electromagnetic wave absorption. *J. Mater. Sci. Technol.* **2022**, *106*, 108-17. DOI
131. Wu, Y.; Wang, G.; Yuan, X.; Fang, G.; Li, P.; Ji, G. Heterointerface engineering in hierarchical assembly of the Co/$Co(OH)_2$@carbon nanosheets composites for wideband microwave absorption. *Nano. Res.* **2023**, *16*, 2611-21. DOI
132. Hu, R.; Luo, J.; Wen, H.; et al. Enhanced electromagnetic energy conversion in an entropy-driven dual-magnetic system for superior electromagnetic wave absorption. *Adv. Funct. Mater.* **2025**, *35*, 2418304. DOI
133. Zhang, X.; Zheng, Q.; Chen, W.; et al. Nanoarchitectonics of RGO-wrapped CNF/GO aerogels with controlled pore structures by PVA-assisted freeze-casting approach for efficient sound and microwave absorption. *Chemistry* **2023**, *29*, e202202714. DOI PubMed
134. Li, Y.; Yun, K.; Yi, X.; et al. Reduced graphene oxide-based magnetoelectric composites for efficient microwave absorption: state of the art and prospects. *Carbon* **2025**, *244*, 120719. DOI
135. Tian, Y.; Zhi, D.; Li, T.; et al. Graphene-based aerogel microspheres with annual ring-like structures for broadband electromagnetic attenuation. *Chem. Eng. J.* **2023**, *464*, 142644. DOI
136. Li, Y.; Guo, S.; Li, Y.; et al. Electrostatic-spinning construction of HCNTs@$Ti_3C_2T_x$ MXenes hybrid aerogel microspheres for tunable microwave absorption. *Rev. Adv. Mater. Sci.* **2023**, *62*, 20230339. DOI
137. Wu, F.; Hu, P.; Hu, F.; et al. Multifunctional MXene/C aerogels for enhanced microwave absorption and thermal insulation. *Nanomicro. Lett.* **2023**, *15*, 194. DOI PubMed PMC
138. Zhang, Y.; Xie, Y.; Yang, W.; Wu, G.; Chen, S.; Wang, Y. Multidimensional and hierarchical design of biomass-derived carbon nanofiber networks for efficient microwave absorption. *Colloids. Surf. A. Physicochem. Eng. Asp.* **2024**, *696*, 134270. DOI
139. Liu, X.; Ma, W.; Yang, T.; et al. Multilevel heterogeneous interfaces enhanced polarization loss of 3D-printed graphene/$NiCoO_2$/selenides aerogels for boosting electromagnetic energy dissipation. *ACS. Nano.* **2024**, *18*, 10184-95. DOI
140. Liu, X.; Zheng, B.; Hua, Y.; et al. Ultralight MXene/rGO aerogel frames with component and structure controlled electromagnetic wave absorption by direct ink writing. *Carbon* **2024**, *230*, 119650. DOI
141. Jiang, B.; Shang, J.; Li, N.; Wang, Y.; Hu, Z.; Yu, J. Aramid honeycomb composites filled with rGO/BC aerogel for broadband microwave absorption and multifunctional applications. *Compos. Commun.* **2025**, *58*, 102512. DOI

142. Wang, Z. Y.; Li, Z. C.; Li, B.; et al. Functional carbon springs enabled dynamic tunable microwave absorption and thermal insulation. *Adv. Mater.* **2024**, *36*, e2412605. DOI PubMed
143. Zhao, H.; Yang, X.; Sun, J.; et al. Biomass-derived oriented carbon aerogels with integrated high-performance microwave absorption and thermal insulation. *J. Mater. Sci. Technol.* **2025**, *226*, 196-204. DOI
144. Wei, H.; Lei, T.; Li, W. Lightweight, flexible, heat resistant and thermal insulating aramid nanofiber/magnetic carbon nanotube interpenetrating network aerogel for microwave absorption in complex environments. *Carbon* **2024**, *225*, 119115. DOI
145. Wang, R.; Xu, H.; Chu, G.; et al. Rigid and lightweight $CoFe_2O_4$/carbon nanofibers/polyimide composite aerogel with anisotropic structure for efficient microwave absorption and thermal insulation. *Compos. Sci. Technol.* **2026**, *273*, 111422. DOI
146. Yu, C.; Lin, D.; Guo, J.; et al. Ultralight three-layer gradient-structured MXene/reduced graphene oxide composite aerogels with broadband microwave absorption and dynamic infrared camouflage. *Small* **2024**, *20*, e2401755. DOI PubMed
147. Nie, W.; Wang, B.; Wu, W.; et al. In situ growth medium entropy alloy nanoparticles on the ordered structure carbon nanofiber aerogel for enhanced microwave absorption and infrared stealth properties. *Small* **2025**, *21*, e2503955. DOI PubMed
148. Li, S.; Sun, Y.; Meng, F.; Jiang, X.; Yu, H. Lightweight Fe_3O_4/Fe/C/rGO multifunctional aerogel for efficient microwave absorption, electromagnetic interference shielding, hydrophobicity and thermal insulation. *Chem. Eng. J.* **2024**, *498*, 155405. DOI
149. Liu, T.; Huang, L.; Wang, X.; Li, Y.; Yuan, Y. A rare-earth oxide@carbon nanofiber aerogel for self-cleaning, infrared thermal camouflage and high-efficiency microwave absorption. *J. Mater. Res. Technol.* **2023**, *25*, 2676-89. DOI
150. Tang, Y.; Shao, S.; Guo, C.; et al. Multifunctional ultralight magnetic Fe_3O_4@SiO_2/Ti_3C_2T/rGO aerogel with efficient electromagnetic wave absorption and thermal management properties. *Carbon* **2024**, *228*, 119314. DOI
151. Hou, Y.; Liu, Z.; Wang, Q.; et al. Magnetic graphene composite aerogel for highly efficient electromagnetic wave absorption and anti-corrosion. *J. Mater. Sci. Technol.* **2026**, *251*, 1-10. DOI
152. Zhang, K.; Liu, Y.; Li, X.; Wang, X.; Liu, J.; Liu, X. All-dielectric ultra-broadband microwave absorbing aerogel with optimized dielectric dispersion via dielectric relaxation time regulation. *Adv. Mater.* **2025**, *37*, e2506386. DOI PubMed